Cities 118 (2021) 103393

Contents lists available at ScienceDirect

Cities

journal homepage: www.elsevier.com/locate/cities

City profile

The story of five MENA cities: Urban growth prediction modeling using remote sensing and video analytics

Ahmed Jaad [b], Khaled Abdelghany [a,*]

[a] Department of Civil and Environmental Engineering, Southern Methodist University, P.O. Box 750340, Dallas, TX 75275-0340, United States of America
[b] Faculty of islamic architecture, college of Engineering and Islamic Architecture, Umm Al-Qura University, P.O. Box: 5555 Makkah, Saudi Arabia

ARTICLE INFO

Keywords:
Urban growth prediction
Machine learning
Convolutional neural networks
Video prediction
Remote sensing
Middle East and North Africa (MENA) Region

ABSTRACT

Most urban areas in the Middle East and North Africa (MENA) region have experienced unprecedented growth rates over the past few decades to absorb population increase and hefty migration from surrounding rural and/or politically unstable areas. Such expedited urbanization presents substantial stresses to these urban areas' ecological and financial resources, as well as to the overall well-being of their residents. This paper studies the urban growth pattern in five major cities in the MENA region including Dubai (United Arab Emirates (UAE)), Cairo (Egypt), Doha (Qatar), Casablanca (Morocco), and Riyadh (Kingdom of Saudi Arabia (KSA)). The study adopts a machine learning (ML)-based modeling framework, which integrates remote sensing and computer vision technologies to generate high-fidelity urban growth prediction with limited data requirements. The framework treats successive satellite images for the urban area under study as a video for which a future frame is constructed to present the predicted growth in a specific target year. The methodology is shown to produce growth prediction results that are consistent with previous studies conducted for these five cities. The obtained results are used to derive several recommendations to assist in developing sustainable growth policies for these cities.

1. Introduction

Many urban areas around the globe have reported significant growth rates over the past few decades. The average urbanization rate is estimated to reach more than 50% in most cities by 2050 (Zhou & Chen, 2018). This high rate of urbanization presents substantial stresses to these cities' ecological and financial resources as well as the overall well-being of their residents. Therefore, there are increasing calls to study urban growth, especially in developing countries where this growth is less controlled and could be associated with many undesirable consequences including the formation of slums, high unemployment rates, lack of infrastructure services (e.g., clean water, sewage, transportation, etc.), and vulnerability to epidemic diseases, to name a few. The purpose of urban growth studies is to identify locations and directions of potential growth, assess infrastructure and public service needs, and ensure the integration of new developments with the existing city structure. In addition, urban growth has been studied for deriving effective policies that help achieve sustainable and economically-sound growth patterns.

The Middle East and North Africa (MENA) is one particular region that is characterized by significant urban growth during the past few decades (Gouda et al., 2016). MENA's total population has grown from around 100 million in 1950 to nearly 578 million in 2018, with around 70% of this population concentrated in urban areas (Statista, 2020). Several factors have contributed to this expedited urban growth in the MENA region. For example, most MENA countries very high birth rates compared to those recorded in the rest of the world. The birth rates of most MENA countries are in the upper 20s per 1000 capita, compared to less than 10 births per 1000 capita in most western European countries. In addition, intensive migration from rural to urban areas has occurred in most MENA cities over the years. The modernization of the agriculture sector has pushed for massive population movement seeking alternative economic opportunities in urban areas. Furthermore, the political instability followed the Arab Spring events in 2011 have also forced migration from war zones in countries like Iraq, Syria, Libya and Yemen to safer cities in the region. For example, the city of Amman, Jordan is estimated to host about 0.40 million refugees from Syria and Iraq in addition to approximately 0.30 million Palestinian refugees (International Centre for Migration Policy Development (ICMPD), 2018). Finally, since the boom of the oil industry in the early 1970s,

* Corresponding author.
E-mail addresses: ahjaad@uqu.edu.sa (A. Jaad), khaled@smu.edu (K. Abdelghany).

https://doi.org/10.1016/j.cities.2021.103393
Received 6 April 2021; Received in revised form 29 June 2021; Accepted 22 July 2021
Available online 2 August 2021
0264-2751/

cities in the Gulf countries have attracted large numbers of emigrant workers. It is estimated that the Gulf countries host about 5.0 million expatriate workers from other countries including Egypt, Pakistan, India, Philippines and Bangladesh. With this unpresented increase in the urban population in the MENA region, local authorities in most cities in the region are struggling to adequately plan for sustainable urban growth and provide efficient infrastructure expansion. Unfortunately, most cities in the region are suffering many of the above-mentioned undesirable consequences of such uncontrolled and unsustainable growth.

Considerable effort has been devoted to developing sustainable urban growth plans for cities in the MENA Region (e.g., Hashem & Balakrishnan, 2015; Alqurashi et al., 2016; Mallouk et al., 2019; Aldogom et al., 2019; Ibrahim et al., 2019; Altuwaijri et al., 2019). One main requirement for developing these plans is to obtain high-fidelity prediction of the growth pattern in terms of its direction and intensity under different growth management scenarios. While several urban growth prediction models (UGPM) have been developed during the past two decades (Chaudhuri & Clarke, 2013; Waddell, 2002), most models are assuming controlled growth environments where strict regulations and enforcement are maintained. This assumption limits the suitability of these models to study urban growth of most MENA cities characterized by uncontrolled growth. In addition, in order to properly calibrate and validate these models, they require intensive amount of historical land use, biophysical and socioeconomic data that extends over a relatively long horizon. Obtaining such historical data is a challenge in most countries in the MENA region. Therefore, UGPMs adopted to study urban growth in the region should be capable of providing accurate prediction results with minimum data requirements.

This paper aims to address these challenges by presenting the application of a machine learning (ML)-based modeling framework for urban growth prediction developed by the authors for several cities in the MENA region (Jaad & Abdelghany, 2020). The framework integrates remote sensing and computer vision technologies to produce high-fidelity urban growth prediction with limited data requirements. The developed ML-based UGPM is in the form of a time-dependent autoencoder (TDAE) with imbedded convolutional neural networks. The developed UGPM treats a sequence of satellite images taken over an extended past horizon for the urban area as a video for which a future frame can be predicted, representing the growth in the target year. The model is trained to learn the temporal and spatial growth patterns from the satellite images and use this information to predict the growth for the specified target year. The model is applied to predict the urban growth of five MENA cities including Dubai (United Arab Emirates (UAE)), Cairo (Egypt), Doha (Qatar), Casablanca (Morocco), and Riyadh (Kingdom of Saudi Arabia (KSA)). These selected cities vary in terms of their size, population, historical heritage, level of control applied to their growth, geographical locations, complexity of their structure, and socio-economic characteristics. For example, Cairo is one of the oldest and largest cities in the MENA region. Founded in 969 CE, the city is located at the fork of the Nile's Delta which expands over 175 mile^2 with a total population of about 20.5 M. On the other side of the spectrum, the City of Doha, located on the Gulf coast, which was founded in 1820 and declared as Qatar's capital in 1971. The city has an area of 51 mile^2 with a population that is close to one million. Egypt and Qatar differ significantly in terms of their gross domestic products (GDPs). While an average GDP per capita of about $2600 is reported for Egypt, Qatar's average GDP per capita is near $70,400 (Plecher, 2019).

The research aims at addressing several important research questions as follows. How can recent advances in ML and remote sensing technologies be leveraged to develop high-fidelity UGPMs? What is the performance of these models when applied to cities with diverse characteristics (e.g., size, growth control levels, cultural and historical background, natural growth constraints, etc.)? How can these models be used to determine key factors that influence urban growth? What recommendations can be derived from the performed model applications to inform policy makers and city planners in the MENA region and in other parts of the world? The research work contributes to the existing literature in several ways. First, the paper extends the work presented in Jaad and Abdelghany (2020) to study urban growth of several cities in the MENA region. The model automatically extracts the spatiotemporal growth pattern from satellite images, and hence deviates from most current practices that require intensive biophysical and socioeconomic data for model development. Second, the paper presents a comprehensive model validation by comparing its results with the results obtained from other urban growth studies conducted for the selected cities. Finally, the paper provides recommendations for sustainable urban growth in the MENA region based on the obtained model results.

Several conclusions can be made based on this research effort, which pertain to (a) the developed modeling framework and (b) the performed applications. On the modeling side, we demonstrate that ML technologies could play an important role in addressing complex problems related to studying urbanization in mega cities. In addition, nontraditional data sources sch as satellite imagery is of great value in understanding urban areas' complex spatial and temporal growth patterns. As we illustrate hereafter, treating subsequent satellite images as a video, we have been able to develop a framework that adopts a dynamic encoder to predict the tempo-spatial growth pattern of five cities in the MENA region. This model application resulted in important recommendations that could assist city planners and policy makers to develop sustainable urban growth plans for their cities. For example, the results indicate that there is a strong correlation between the roadway network and the predicted growth in the studied cities. As more priority is often given to developing vacant areas that are accessible by the existing roadway system, the integration of the urban and transportation planning processes becomes critical for ensuring the sustainable growth of these cities. In addition, our analysis provided insight on the effectiveness of ring roads in defining the city boundaries or limiting their growth. While ring roads are effective in alleviating congestion, their ability to control city sprawl has shown to be limited. The results also show that mega projects (e.g., amusement parks, stadia, art districts) could result in significant changes in their surrounding areas, either in terms of new developments or changes in the current land-use patterns. Furthermore, our analysis showed that there are considerable benefits in diversifying housing options within the city to ensure community stability and controlling urban sprawl. Finally, urban growth could occur at the expense of valuable natural resources within or surrounding the city. Thus, there are urgency to develop incentives to prevent development on green areas and ensure green space equity.

This paper is organized as follows. Section 2 provides an overview of the MENA cities selected for this study. Section 3 reviews ML-based models developed to study urban growth prediction and also provides a review of previous urban growth studies conducted for the selected MENA cities. The overall architecture and data requirements of the model adopted in this study are then described in Section 4. The application of the model to predict the growth pattern for the selected MENA cities is then presented in Section 5. Finally, Section 6 concludes with a discussion on best practices to achieve sustainable urban growth for the MENA region.

2. Overview of the selected cities

In this section, we provide an overview of the five MENA cities considered in this study. For each city, we present a brief historical background, growth trends and basic demographic and socio-economic data co INCLUDEPICTURE "https://cdn.statcdn.com/Topic/1630.jpg" * MERGEFORMATINET ntributing to the growth. Fig. 1 gives a map showing the location of these cities in the MENA region along with a summary of their characteristics. Fig. 2 shows the maps of these cities along with their population growth trends from year 1984 to 2019.

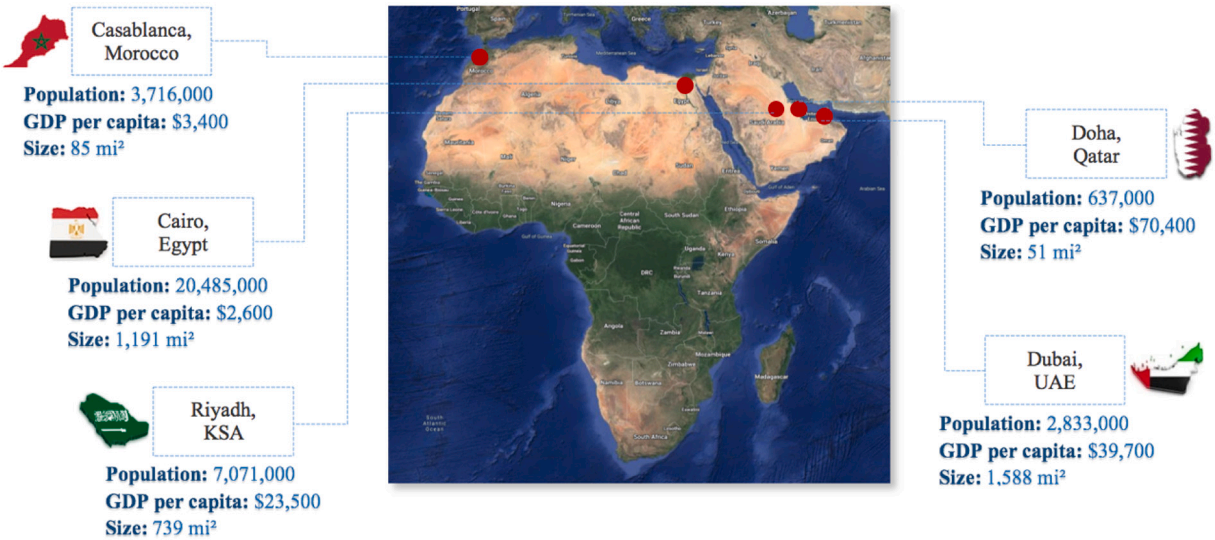

Fig. 1. The five MENA cities considered in this study.

2.1. Dubai, UAE

Located on the coast of the Persian Gulf in the Arabian Peninsula, Dubai is UAE's second-largest city after Abu Dhabi and the most crowded city in UAE (Held & Cummings, 2018). The city was first established in the early years of the nineteenth century (Ulrichsen, 2016). Modern development of the city started with the oil boom in 1960's. The city covers about 1600 mile^2, representing 5.0% of the total area of UAE. With an average GDP per capita of about $39,700, the city is one of the richest cities in the region. Dubai is a perfect example of rapidly developing cities. The city's population has grown significantly over the past four decades. In 1984, the total population was only 325,000 capita, which jumped to more than 2.8 million capita in 2019. The city was gradually transformed from a small cluster of settlements on the Gulf into a modern multicultural city with a state-of-the-art infrastructure and commercial hubs. According to Elessawy (2017), the progress of Dubai's urban development could be divided into four different periods: (1) urban origin before 1971, (2) the planned suburban growth from 1971 to 1984, (3) the modern construction of Dubai from 1985 to 2003, and (4) the mega city formation starting in 2004. In the first period, Dubai Municipality was established and started to form the roads and the town center following the city's first master plan. During this period, growth has sprawled incoherently on the outer edges of Dubai specifically along the West roads towards the city of Abu Dhabi and the East roads towards the city of Sharjah. A new master plan was developed for the second period followed by enormous expansion, where the total built-up area increased from 15.44 to 42.08 mile^2 (Elessawy, 2017). In the beginning of the third period, a strategic plan was created to guide the development of the city into the 21st century. The plan included the construction of mega projects converting the city into a large metroplex with city-of-cities structure, where the city's total built-up area expanded to about 380 mile^2. The current stage focuses on the upgrade of the city's central business district (CBD) and the construction of new suburbs. Enriching the city's skyline, several hotels, residential and financial tower buildings have been constructed, which contribute significantly to the city's economic and tourism activities. Peripheral growth also continued to occur, connecting the city to adjacent emirates such as Sharjah and Ajman to the east and Abu Dhabi to the west.

2.2. Cairo, Egypt

Cairo is Egypt's capital and considered the most significant urban center in Africa due to its long history and large population. The city is located at the fork of the Nile's Delta north of Egypt. The city covers about 1191 mile^2 on the east and west banks of the River Nile and is surrounded by desert hills to the east and west (New World Encyclopedia, 2016). As one of the most crowded cities in the world, Cairo's current population is estimated at about 21 million with a current growth rate close to 2%. Modern Cairo was founded as a capital by the Fatimid dynasty in 969 CE, and since then the city has undertaken several stages towards urbanization (AlSayyad, 2013). The urban development of Cairo was based on the idea of asserting its significance and developing a highly accessible capital. As such, the construction of highways and bridges in the city center allowed smooth connection between the new housing areas and the city's commercial center. In addition, new highways were constructed along the east-west axis, which serve the city's central business district and connect the airport to the pyramids of Giza. To accommodate the significant increase in the population, a plan was envisioned to develop new societies in the dessert surrounding the old city. The government established several new towns in the desert to facilitate urban growth outside Cairo and its agricultural periphery. However, some of these towns failed to attract considerable population because they lacked the necessary services and infrastructure. In the last two decades, private developers were handed over the business of new residential developments in Cairo and the new surroundings towns. However, private developers focused on building new compounds that serve mainly the high-income sector which represents a small percentage of the population. Most recently, the government started the construction of a new administrative capital in the desert east of Cairo. The new city is expected to host the government offices and most of the professional and financial services. The dynamics of Cairo in light of the interaction between the old and the new capitals are to be revealed in the coming years.

2.3. Doha, Qatar

Since the establishment of the State of Qatar in 1971, Doha was declared as the country's capital and quickly became the center of most its economic and cultural activities. The city occupies about 51 mile^2 on the east coast of Qatar Peninsula. It has gradually transformed from a small pearling and fishing settlement to a modern urban center. Doha's population has grown significantly over the past few decades reaching near 0.65 million capita in 2019, compared to about 50,000 in 1971. The city is also the destination of a significant number of foreign workers, representing about 40% of the total population. In the early stages of the city, Doha's urban development was based on transit-

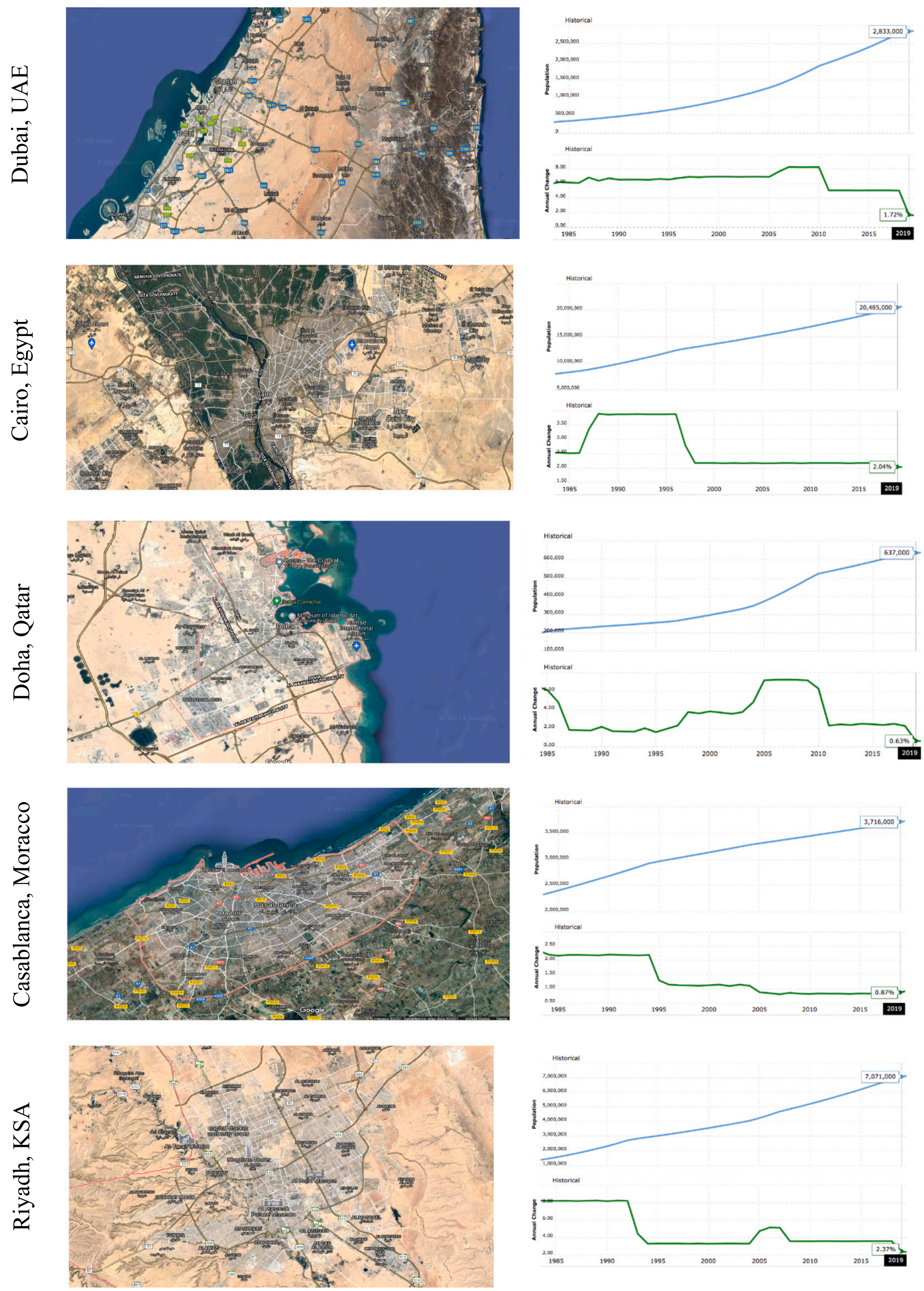

Fig. 2. The studied cities and their population growth and rate of change trends (1984–2019).

oriented development supported by a streetcar and railway system (Zaina et al., 2016). With the boom of the oil and gas industry, more dependence on the private car has been observed, resulting in significant sprawl to accommodate the high rate of population growth. The country's strong economy enabled the construction of new shopping malls, neighborhoods, and other facilities that have entirely reshaped Doha into a modern capital (Azzali & Tomba, 2018). Mega infrastructure projects are undergoing as the country is scheduled to host the FIFA's World Cup activities in 2022.

2.4. *Casablanca, Morocco*

A coastal city located on the Atlantic Ocean, Casablanca is one of the oldest cities in North Africa. The city occupies about 85 mile^2 in western Morocco with a population that is close to 3.8 million capita. The city is known as Morocco's second capital and a significant tourist attraction. For several decades, the city continued to operate as a small-sized harbor with the population gradually stretching due to the improved residential homes and increased economic opportunities. The first master plan for promoting the urban development of the city was developed soon after the French occupation in 1907 (Folkers & Buiten, 2019). The plan consisted of two main phases. The first phase focuses on reestablishing the city as a great port situated near its traditional core. The later phase suggested establishing a modern city to be developed around the city core. In the past few decades, the city has experience significant population growth resulting mainly from migration from surrounding farming areas. With an estimated average GDP per capita of about $3400 by the end of 2020, the government has been struggling to develop the city to cope with this significant population increase. Despite effort to maintain controlled zoning practice to prevent undesirable growth patterns, the city of Casablanca has seen the formation of several slum areas occupied mainly by migrated agricultural labor from the mountains area. In recent years, the government has attempted to stop further growth of these slums by constructing large-scale social housing projects, offered to the residents of these slums and other low-income groups. In addition, the private sector started to become involved in the city development with several ongoing projects to remodernize the traditional city core by adding affordable apartment complexes.

2.5. Riyadh, KSA

Riyadh, the capital of KSA, is located in the middle of the Arabian Peninsula. Similar to most cities in the rich gulf countries, Riyadh is one of the few cities in the world whose urban developments have transformed significantly over a short period. The city evolved from a small desert village in the beginning of the 19th century to a large metropolitan area with more than seven million residents. Since the establishment of the Kingdom as an independent state in 1932, the city has been used as the government headquarters and declared as the Kingdom's new capital. Taking advantage of the country's oil-trading wealth, the government has implemented significant projects to modernize the city, focusing on infrastructure development. In early stages, the city was growing in all directions with expedited establishment of neighborhoods of single-family houses. A master plan was later developed for the city suggesting the establishing a north-south axis to allow for future growth (Elsheshtawy, 2019). The plan did not consider public transportation, assuming full dependence on private vehicles as the sole mode of transportation. The city continued to grow in all directions, suffering from an uncontrolled urban sprawl pattern. With the increasing traffic congestion problem, the city pushed for more investment in public transportation. Projects are underway to construct the city's metro network to reduce dependence on the private car and the associated congestion problem.

3. Literature review

In this section, we review research work focusing of UGPM development using machine learning techniques, similar to the one adopted in this paper. Next, we review studies focusing on urban planning and growth prediction of the five selected MENA cities.

3.1. Machine learning based urban growth prediction models

Previous studies have resulted in numerous UGPMs that differ in their underlying theory, data requirements, and scope of application. According to Triantakonstantis and Mountrakis (2012), the main objective of UGPMs is to capture the fundamental relationships of spatial and temporal complexities associated with urban growth prediction. While many approaches have been proposed for developing UGPMs, those that adopt ML techniques have considerably attracted the attention of the research community in the past two decades. Examples of ML techniques that have been used to develop UGPM include Artificial Neural Network (ANN), Cellular Automaton (CA), and Linear/Logistic Regression (LR), which have generally demonstrated superior performance compared to other explored techniques (e.g., decision trees and fractals analysis).

For example, the ANN technique has been widely adopted in modeling land use change and urban growth prediction (e.g., Lin et al., 2011; Shafizadeh-Moghadam et al., 2017; Tayyebi & Pijanowski, 2014). One advantage of ANN over classical regression analysis is that it does not require pre-specification of the relationship between the independent and dependent variables. ANN models are trained using the backpropagation algorithm following an iterative procedure to determine the optimal weights that minimize the difference between the training data and the estimated output (Chauvin & Rumelhart, 2013; Zhang & Goh, 2016). Several rigorous ANN-based models with rich socioeconomic and environment input data for studying complex urban growth patterns have been developed in the past two decades (Berling-Wolff & Wu, 2004). For example, Liu and Seto (2008), Thapa and Murayama (2009), and Tayyebi et al. (2011) developed an ANN-based model with input data that includes topology, land use, and roadway network extracted from satellite images to predict city boundaries and developed areas within these boundaries. ANN-based models have also been integrated with geographic information system (GIS) tools to provide forecast and visualize changes in land use (Pijanowski et al., 2005). The CA technique is also widely adopted in developing UGPMs considering its relative simplicity (He et al., 2006). CA represents complex dynamic environments in the form of a grid of cells that interact with each other according to predefined rules. These rules are extracted from historical growth observed for the urban area under study or for other similar urban areas. Several case studies are devoted to demonstrating the application of CA-based UGPM (Chaudhuri & Clarke, 2013; Clarke & Gaydos, 1998; Ke et al., 2016; Van Vliet et al., 2009). According to Chaudhuri and Clarke (2013), one of the popular CA-based UGPM is the SLEUTH (slope, land cover, excluded, urban, transportation, and hillshade) model, which is used to explain the growth phenomena observed in many cities around the world. Finally, several LR-based models are proposed for developing UGPMs (Gerasimovic et al., 2016; Han & Jia, 2017). LR is useful for driving a relationship that explains the urban change, in the form of a binary variable, in terms of different explanatory variables. For example, Han and Jia (2017) developed UGPMs in the form of LR that combines variables such as socioeconomics, land topology, land zoning, and accessibility to the city center. The LR model developed by Mustafa et al. (2017) is shown to present the growth in commercial developments as a function of the evolution of the roadway network and changes in property taxes.

3.2. Urban growth studies for the considered MENA cities

3.2.1. Dubai

Several recent studies have focused on studying the progression of the city of Dubai. These studies incorporate both remote sensing (RS) and GIS (Alghais, 2018). For example, Khalil et al. (2017) adopted a technique to assess the city's infrastructural growth by analyzing a sequence of satellite images. Elmahdy and Mohamed (2018) proposed a low-cost remote sensing (RS) approach to analyze the land use and land cover (LULC) changes. Their methodology adopted an image difference procedure to improve the categorization of maps and aid the process of growth monitoring and evaluation. The study predicted a considerable reduction in the vegetation cover in the city as a result of urbanization. Adopting a methodology similar to the one presented in Khalil et al. (2017), Aldogom et al. (2019) employed multiple time series Landsat images to discover and evaluate the city's development profile. The methodology consists of three main steps. The first step involved classification algorithms in conjunction with variation detection, segmentation, and extraction to achieve LULC footprints. In the second step, Shannon's entropy is used to predict if the city is compacting or sprawling. In the third step, the CA-Markov approach was applied to simulate the city's future expansion. The study reported a significant evolution in the urban fabric of the city, estimating a 3% expansion by 2030 at the expense of green areas and open spaces. Similar results were reported in the model adopted by Abulibdeh et al. (2019).

3.2.2. Cairo

Several studies have focused on studying Cairo's growth focusing on developing sustainable growth plans for the city. The work of Abdalmalak and Gonzalez-Serrano (2016) and Midekisa et al. (2017) discuss the derivers of uncontrolled growth in Cairo and the need to address them for sustaining and protecting surrounding farming spaces. Osman et al. (2016) evaluated policies to preserve agricultural space on the north and the south borders of the city. They employed the SLEUTH model to analyze the influence of the policies on land use. The model provided two conclusions: a) a compact growth approach could pose minimal effect on the agricultural space, and b) the city will continue to grow considering its historical expansion trends. In a subsequent effort, Osman et al. (2019) developed a modeling framework that integrates Markov Chain (MC), CA, and Logistic Regression (LR). The framework aimed at enhancing the value of spatiotemporal models and extrapolations of urban sprawl and land utilization variations. The framework predicted a continuous loss of agricultural land, and the development of future urban settlement along major roads. Ibrahim et al. (2019) developed PredictSLUMS, an ML-based model developed to identify and forecast the expansion of unofficial settlements in Cairo. PredictSLUMS integrates Multinomial Logistic Regression (MLR) and ANN techniques. The model displayed a high legitimacy and precision in identifying and forecasting informal growth within Cairo.

3.2.3. Doha

Several models have been developed to study the process of urbanization and inform sustainable land use management and policy-making for the city of Doha. These studies emphasized that the expedited logistic and infrastructure projects within the city significantly affected its urban fabric as a result of poor realization of master plans and land utilization strategies (Mansour et al., 2020; Verbeek, 2017). Shandas et al. (2017) developed a model to evaluate the opportunities for sustainable growth based on remote sensing data. They examined the pace, quality, and behavior of expansion. The outcome of their study suggested that the development patterns of Doha were equivalent to that of western cities. As such, urban planners need to evaluate if this growth pattern can be sustainable. The model developed by Makido et al. (2020), which is based on a mixture of spatial analysis, predicted that more than 20,000 ha of open space will experience urban developments. The study suggested that this scenario could significantly change the land utilization patterns and impact the overall environment quality of the city. Hashem and Balakrishnan (2015) proposed a model that is based on Markov process integrated with GIS and remote sensing to generate different scenarios of future LULC change in the city. The model predicted that the built-up areas will increase by about 20%, occurring in the urbanized open space within and around the city.

3.2.4. Casablanca

Concerned by the city's ongoing uncontrolled growth, several models have been developed to enable informed decision making by policy-makers and planners (Bugday & Bugday, 2019; Kadhim et al., 2016). For example, Mallouk et al. (2019) developed an urban growth prediction model that is based on the SLEUTH model. The approach entails calibrating the model using data extracted from historical satellite imagery. The result of the study predicted an increase in the urbanized space as a result of expanding the city's port infrastructure. Saadani et al. (2020) developed a CA-based Markov Chain (CA-MC) approach to simulate the growth of Moroccan cities. The model combined CA-MC with Landsat images to forecast LULC. The study reported that rapid urban growth did replace the agricultural spaces. The prediction outcome calls for the institution of novel environmental protection measures and the promotion of sustainable growth.

3.2.5. Riyadh

Several models have been used to explain the growth pattern of the city of Riyadh. For instance, Al-Ahmadi et al. (2016) presented an improved CA-based model referred to as Fuzzy Cellular Urban Growth Model (FCUGM) that incorporated a genetic algorithm (GA), parallel simulated annealing (PSA), and expert knowledge (EK). The outcome of this study suggested that a combination of GA and EK enhances the model's prediction performance. Alqurashi et al. (2016) used a simulation model that integrates the CA and MC techniques to predict the urban growth at years 2024 and 2034, respectively. Their model is claimed to offer a fundamental comprehension of historical, present, and future patterns of urban sprawl in the city. Al-Ahmadi (2018) modeled the expansion pattern and the derivers of urbanization in the city of Riyadh by incorporating GIS and Fuzzy sets. The results obtained by the model are intended to simulate the decision-making process utilized for zoning and defining land use structures. The study conducted by Altuwaijri et al. (2019) focused on predicting the growth of the city to year 2040 using the CA-MC model supported by GIS platform. The study predicted 38% increase in urban spaces during the next three decades. Finally, Alghamdi and Cummings (2019) used the high-resolution SPOT 5 images and developed a framework that integrates maximum likelihood and object-oriented categorization to assess land use variation between years 2004 and 2014.

4. Urban growth prediction modeling: a computer vision approach

Two important technologies have significantly benefited the ongoing UGPM development effort: (I) satellite imagery and (II) computer vision. Satellite imagery has been widely used as a reliable data source for UGPM development (Ayazli et al., 2019; Gómez et al., 2020; Liang et al., 2020; Weng, 2002). It provides information on change of land cover over time, and hence can be used to retrieve reliable information on the time-varying growth pattern in urban areas. The usage of these images has been limited mostly to manual data extraction for the purpose of model calibration and validation. However, the improved quality of the satellite imagery datasets enables more comprehensive usage of these images to develop the next-generation UGPMs. These models could automatically learn the spatiotemporal growth pattern from the satellite images and use the learned pattern to predict the growth for future years. In a parallel effort, numerous computer vision-based models have been developed over the past decade focusing on many applications, such as medical (Black et al., 2020; Kalinin et al., 2020; Kaur & Khosla, 2020), defense (Husodo et al., 2019; Qiu et al., 2019; Ye et al., 2020), emergency response (Cho et al., 2019; Li et al., 2019), driverless vehicles (Chen et al., 2020; Joubert et al., 2020; Thakurdesai & Aghav, 2020), infrastructure management (Choi & Dyke, 2020; Hashemi & Abdelghany, 2018; Wang et al., 2020), and infrastructure health monitoring (Acharya et al., 2018; Bang et al., 2019; Gao & Mosalam, 2018; Li et al., 2019; Rafiei & Adeli, 2018). These models take advantage of recent computational advances and the ability to obtain high quality imagery data. In particular, deep learning (DL) techniques have enabled the development of advanced computer vision models with unprecedented capabilities of extracting and memorizing complex features in images precisely and efficiently (He et al., 2016; LeCun et al., 2015; Schmidhuber, 2015).

This section describes the model developed by Jaad and Abdelghany (2020), which is applied in this study to predict the growth pattern for the five MENA cities mentioned above. The model adopts a video prediction approach, which treats successive satellite images taken for an urban area over an extended horizon as a video. The model aims at predicting future frames of that video based on the temporal and spatial features learned from its past frames, as illustrated in Fig. 3. The developed video prediction model is in the form of a TDED with embedded CNNs Vukotic et al. (2017) and Tatarchenko et al. (2016). The model is trained to learn the spatiotemporal growth features from

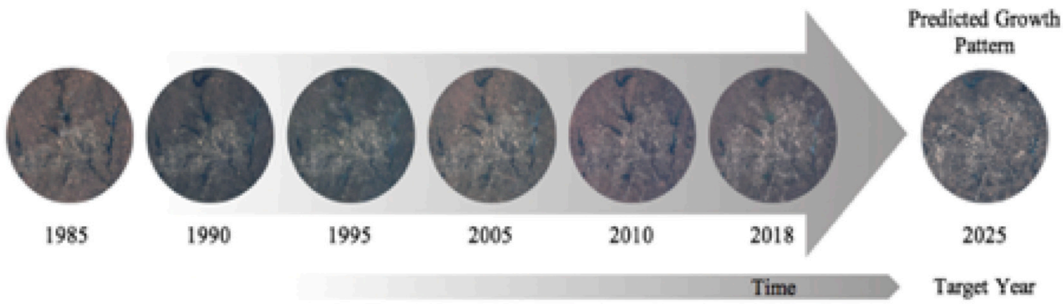

Fig. 3. A video prediction paradigm for urban growth prediction modeling (Jaad & Abdelghany, 2020).

the satellite images, which enables it to predict the growth pattern in the urban area for a given future year. The input of a trained model includes: (a) a base-year satellite image with a pre-defined resolution for the urban area under study; and (b) the length of the prediction horizon of interest (i.e., target year). As an output, the model constructs an image that predicts the growth pattern for the urban area for the target year or any other year within the specified horizon.

Fig. 4 presents the overall structure of the model. As shown in the figure, the model consists of two main components: encoder and decoder. The encoder receives two input elements. The first input is the base-year satellite image for the urban area under study with a pre-defined resolution. The second input is the length of the prediction horizon of interest, Δt (i.e., desired temporal movement). The input image is processed through the encoder which includes a series of convolutional and pooling layers. The first convolutional layer in the encoder defines the resolution of the input image (height, width, and color channels). The last layer in the encoder is connected to a fully connected neural network, FC1, that encodes the image information. The time horizon input is directly encoded into two consecutive fully connected networks, FC0′ and FC1′, respectively. The two fully connected networks FC1 and FC1′ are then concatenated forming one fully connected network, FC2, that combines the image and the time horizon information. The decoder component is responsible for decoding the information in FC2 to generate the predicted image for the specified time horizon. As shown in the figure, the decoder follows a reverse structure of the encoder through implementing a series of de-convolutional and up-sampling (unpooling) layers to construct an image for the target year with the same resolution as that of the input image. Table 1 gives more details on the composition of the layers used to construct the encoder and the decoder, respectively. In the current implementation, a colored image with 512 × 512 × 3 resolution is processed using five convolutional layers with 1 × 1 strides in each layer and five maximum pooling layers. These layers transform the input tensor to a tensor of size 16 × 16 × 256. This tensor is processed through a dense network of dimension 16 × 16×256. The time horizon is encoded into another tensor with dimensions 16×16×1. Thus, a concatenated tensor with dimensions 16×16x257 is obtained. The decoder consists of five deconvolution layers and five unpooling layers which decode the concatenated input tensor to produce the predicted image with 512 × 512 × 3 resolution.

To train and validate the model, a dataset is prepared for the study area under consideration. Each record in this dataset is defined in terms of the triplet I_x, I_y and Δt, where I_x represents the input image at time t_0, I_y represents the target year image at time $t_0 + \Delta t$, and Δt is the time difference in years between the two images. Each data record could have a different time period depending on the years of I_x and I_yIy. The two images I_x and I_y have the same resolution. Once the model is trained and validated, it can be used to construct a predicted image I_y for a given input pair I_x and Δt. For the purpose of applying the model to predict the growth pattern for the urban area under consideration, I_x is typically taken as the image of the current year. Nonetheless, for the purpose of model validation and testing, I_x could be any image with time index t_0 such that a subsequent image I_y with time index $t_0 + \Delta t$ exists in the

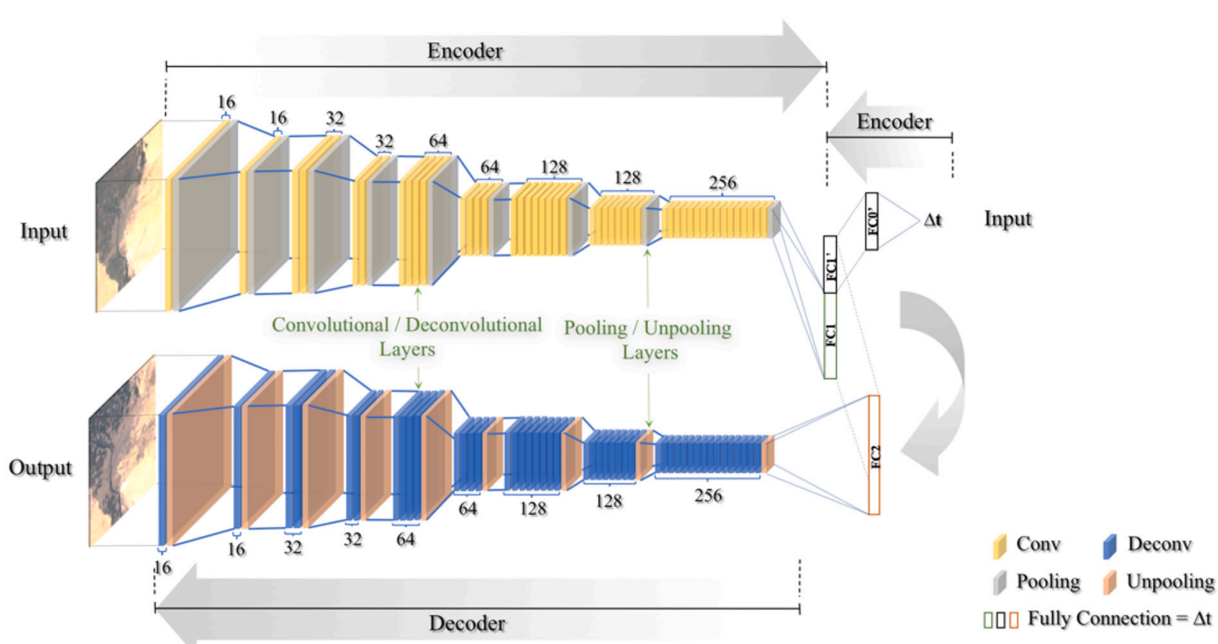

Fig. 4. The overall structure of the time-conditioned encoder-decoder architecture for UGPM.

Table 1
The dimensions of the different layers of the encoder-decoder architecture (Jaad & Abdelghany, 2020).

Layer ID	Layer type/ activation	Kernel size	Strides	Filter	Spatial input size	
	Encoder					
	Input_1 (512 × 512) RGB image					Input_2 (Time)
CL1	Conv2D-ReLU	3 × 3	1 × 1	16	512 × 512	FC0′ (time)
	MaxPooling2D					FC1′ (time)
CL2	Conv2D-ReLU	3 × 3	1 × 1	32	256 × 256	Concatenate (FC1, FC1′ (time))
	MaxPooling2D					FC2
CL3	Conv2D-ReLU	3 × 3	1 × 1	64	128 × 128	
	MaxPooling2D					
CL4	Conv2D-ReLU	3 × 3	1 × 1	128	64 × 64	
	MaxPooling2D					
CL5	Conv2D-ReLU	3 × 3	1 × 1	256	32 × 32	
	MaxPooling2D					
	FC1					
	Decoder					
DL5	Deconv2D-ReLU	3 × 3	1 × 1	256	16x16	
	UpSampling2D					
DL4	Deconv2D-ReLU	3 × 3	1 × 1	128	32 × 32	
	UpSampling2D					
DL3	Deconv2D-ReLU	3 × 3	1 × 1	64	64 × 64	
	UpSampling2D					
DL2	Deconv2D-ReLU	3 × 3	1 × 1	32	128 × 128	
	UpSampling2D					
DL1	Deconv2D-ReLU	3 × 3	1 × 1	16	256 × 256	
	UpSampling2D					
	Output (512 × 512) RGB image					

dataset. The image constructed by the model, $\widehat{I}_y$, is then compared to the ground truth image, I_y, and their similarity measures are reported (Wang et al., 2004). The model is implemented using the Keras-TensorFlow platform (Brownlee, 2016; Shanmugamani, 2018). Keras is an open-source neural-network library that is written in Python and runs on top of TensorFlow, which is also an open-source software library that enables fast implementation of deep neural network models. A sensitivity analysis is conducted to determine the model's optimal settings and values of its hyperparameters including number of layers in the TDED architecture, optimizer, data size, number of epochs and batch size. The model recorded the highest performance when the RMSprop optimizer with 2000 epochs and 64 batch size was used considering TDED with five convolution layers and five deconvolution layers as presented in the table above. As an additional validation exercise, the developed model was successfully applied to predict the growth pattern for the Dallas-Fort Worth (DFW) region focusing on two of its fast-growing counties (Collin County and Denton County, two of the fastest growing counties). The prediction results of these models are compared against the growth pattern predicted by North Central Texas Council of Government (NCTCOG), the metropolitan planning organization for the DFW area (The G-LUM Model, 2009; The UPLAN Model and Data, 2001). More details on the model validation effort and its application to the DFW region can be found in Jaad and Abdelghany (2020).

5. Urban growth prediction for the selected MENA cities

This section presents the results of applying the ML-based urban growth prediction model described in the previous section for the five selected MENA cities. Here, we adopted the same model structure and hyperparameter values used for the DFW model developed in Jaad and Abdelghany (2020) (i.e., autoencoder with five convolution and five deconvolution layers, RMSprop optimizer, 2000 epochs, and 64 batch size). The model is trained using a dataset obtained for each of the five cities. In other words, a sperate model is developed for each city using its satellite imagery dataset. To prepare the dataset for each city, a series of historical satellite images for that city is first collected. High resolution images became available starting in year 1984 with the launching of Landsat 5 (U.S. Geological Survey, 2020). Thus, a past horizon that extends from 1985 to 2019 is considered. The clearest image in each quarter of each year is obtained. In cases where there are no clear images (i.e., cloudy conditions) available for a quarter, an image from the next or previous quarters is borrowed for that quarter. Thus, four different streams of satellite images are obtained for each area. Each stream includes 35 images that represent the area's year-to-year growth. Each stream resulted in 765 data records (i.e., combinations of I_x, I_y, Δt). Combining the four streams together, a total of 3060 data records are obtained for each city. This dataset is used for model training and validation with 80%–20% split. A high-performance computing (HPC) cluster with graphics processing capabilities is used to train the model. The cluster includes 36 cores of NVIDIA P100 GPUs with 256 GB memory. It is worth mentioning that the downloaded satellite images have a resolution of about 15,000 × 12,000. However, these high-resolution images could not be used directly considering the limited memory of the used HPC platform. The downsizing of the images is conducted in an iterative way. After several trials to examine the highest resolution that can be used, the resolution of the original images was reduced to 512 × 512.

Fig. 5 illustrates the convergence pattern of the accuracy and loss functions for the training and validation processes of the model developed for each city. As illustrated in the figure, all five models showed systematic conversion patterns of their accuracy and loss functions. A summary of the values of these functions at convergence is also given in Table 2. As shown in the table, all models converge at accuracy value higher than 94.00% and loss value that are less than 0.002. For example, the city of Riyadh recorded the highest accuracy value at 99.39%, and the lowest loss value at 0.001. On the other hand, the city of Casablanca recorded the lowest accuracy value at 94.19%, and the highest loss value at 0.0019.

Considering year 2019 as the base year, the model is used to predict the growth patterns for the five MENA cities in the target year 2026, respectively. While the model can cover longer horizons, the dataset prepared for model training (combinations of I_x, I_y, Δt) is expected to have more observations with small Δt values compared to those obtained for large Δt values. Thus, a prediction horizon $\Delta t = 7$ is considered as it captures the tradeoff between using longer prediction horizons and having enough observations in the data to adequately learn the growth pattern for this horizon. The prediction is obtained in the form of a model-constructed satellite image showing the city growth in the target year.

Figs. 6 to 10 present the obtained prediction results for the five cities. In each figure, the constructed satellite image is given for the target year. In addition, the difference between the target year's image and the base year's image is provided. This difference image highlights all zones predicted to include significant growth activities (i.e., zones with significant difference between the predicted and the base images). To validate the obtained prediction results, each figure included a zoom-in view of each identified growth zone showing its current state of development. Examining these zoom-in views shows that these zones are either an extension of existing developments located at the city boundaries, or a fill of an open space surrounded by already developed

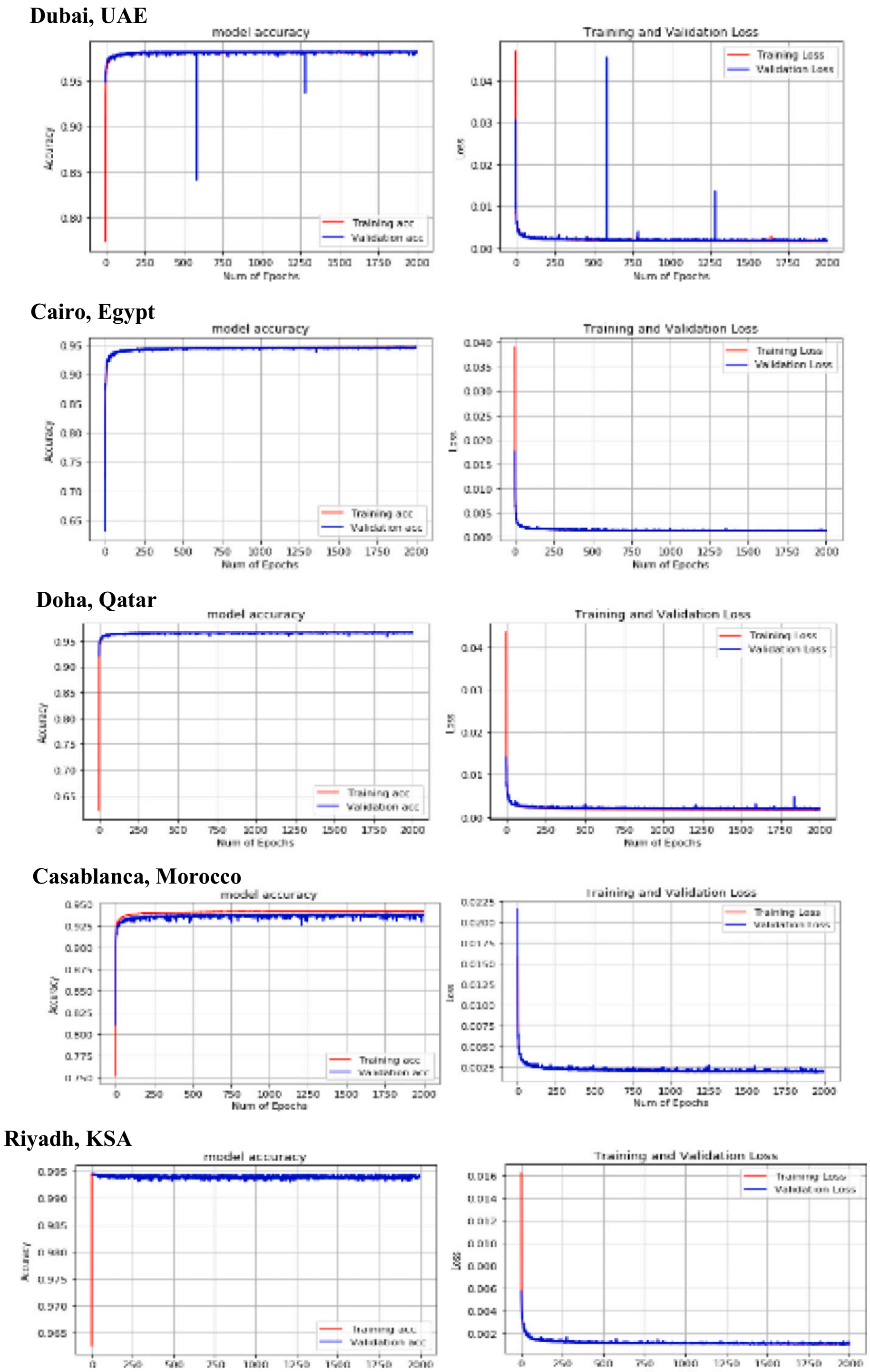

Fig. 5. The convergence pattern of the accuracy and loss functions for the model's training and validation processes for the five MENA cities considered in this study.

Table 2
The model prediction performance for five MENA cities.

MENA cities	Training		Validation	
	Accuracy	Loss	Accuracy	Loss
Dubai, UAE	0.9814	0.0016	0.9820	0.0017
Cairo, Egypt	0.9467	0.0012	0.9468	0.0012
Doha, Qatar	0.9663	0.0017	0.9665	0.0020
Casablanca, Morocco	0.9419	0.0019	0.9382	0.0019
Riyadh, KSA	0.9939	0.0010	0.9938	0.0010

areas. In all cases, these identified zones are located near major roadways that facilitate their access. The following subsections provide an analysis of the results obtained for each city by comparing them with results obtained from previous urban growth studies conducted for these cities. Of course, one should not expect a perfect match between the future growth pattern produced by the model and those obtained from other studies, which themselves are predictions that need to be verified. Nonetheless, the analysis presented here is intended to generally examine the level of agreement between the different modeling approaches.

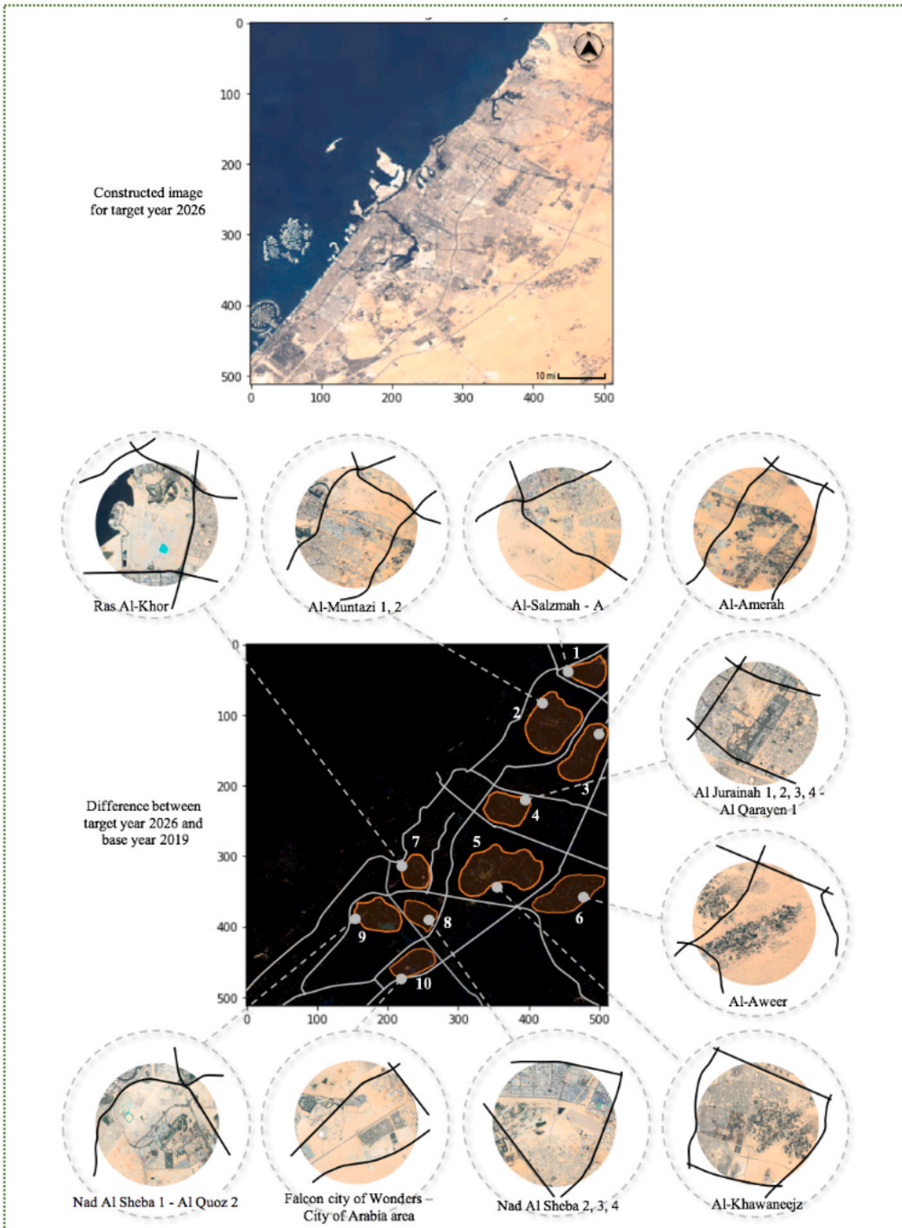

Fig. 6. Predicted urban growth of the city of Dubai for year 2026.

5.1. Dubai, UAE

As shown in Fig. 6, the model predicts 10 zones with active development in the target year. The development of these zones is expected to further convert the cities of Dubai, Sharjah and Ajman into one large metropolitan area and to further expand its size. These 10 zones are a combination of peripheral zones as well as inner zones that were skipped in previous development stages. Zones 1, 6, 9 and 10 are examples of peripheral zones that expand the size of Dubai's metropolitan area. For example, Zone 1 shows a future growth in Al-Salamah and Al-Abrab located on the north and northeast boundaries (i.e., north east of Ajman). Similarly, Zone 9 and Zone 10, are located at the south boundaries of Dubai known by Nad Al Sheba 1, MBR city, Al Quoz 2, and City of Arabia area. Inner zones are partially developed areas with vacant land that is ready for further development as shown in Zones 4, 5 and 7, respectively. The zones representing Al-Jurainah, Al-Khawaneej and Al-Khor areas will experience development to fill their vacant lands. One observation is that all identified growth zones are accessible through the existing roadway network. This pattern demonstrates the strong correlation between transportation accessibility and urban growth. In addition, it is clear from the zoom-in views provided in Fig. 5 that the identified growth zones are surrounded or close to areas that are already developed. New developments that is not connected to the existing fabric of the city has not been observed. As a validation exercise, the results in Fig. 6 are compared against those reported in Aldogom et al. (2019). Unfortunately, this benchmarking study was limited only to the Emirate of Dubai excluding its neighboring cities: Sharjah and Ajman. In addition, the study was also limited to defining the new boundaries of the city without identifying density changes within these boundaries. As mentioned earlier, Aldogom et al. (2019) implemented a methodology that integrates classification algorithms and CA-Markov approach to simulate the city's future expansion for years 2030, 2050, and 2100, respectively. The CA-Markov approach creates a transition probability matrix to evaluate the changes in each pixel in the map over time, and a transition area matrix to illustrate the number of these changed pixels. The results of this study are summarized in Fig. 11,

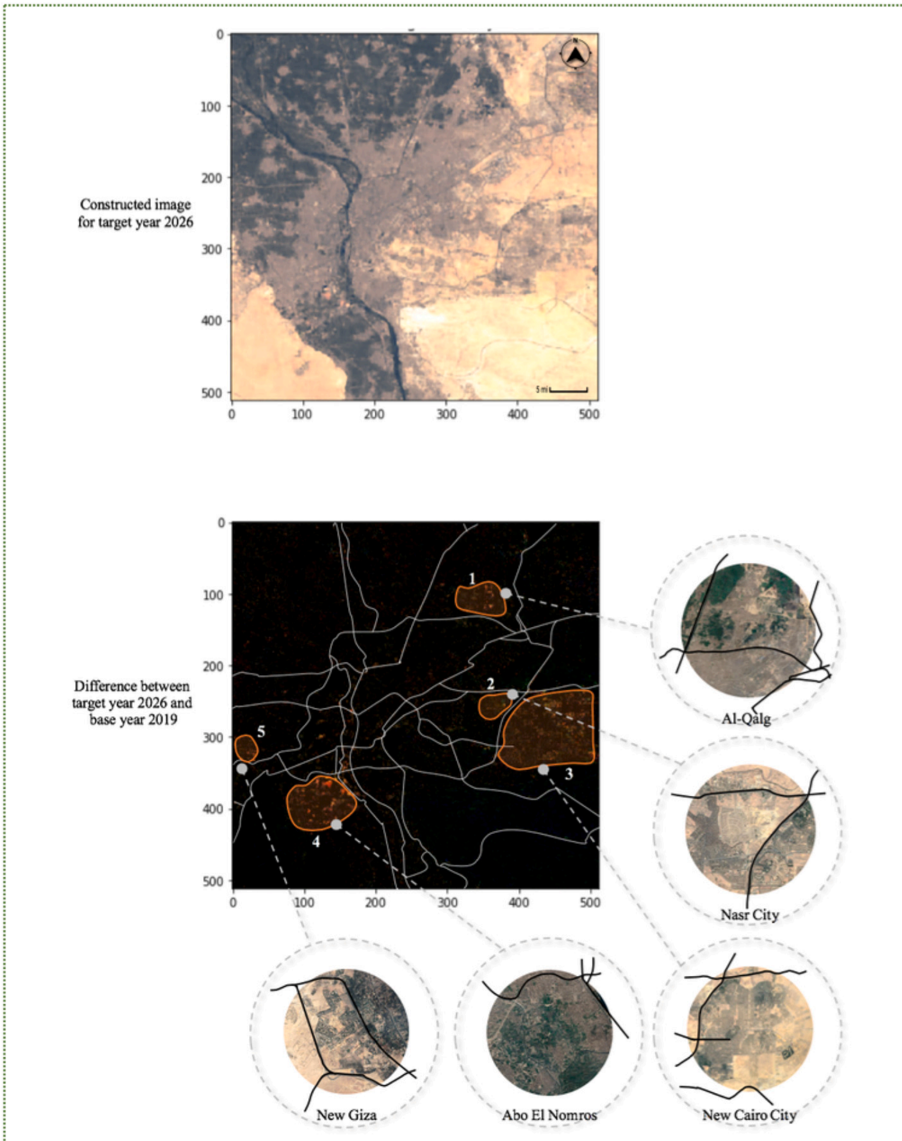

Fig. 7. Predicted urban growth of the city of Cairo for year 2026.

which presents the predicted growth for the three considered target years. The predicted growth zones obtained by our model are superimposed on that figure. The figure shows that the growth zones identified within the borders of the Emirate of Dubai (Zones 5 to 10) are falling within the 2030 city growth reported by Aldogom et al. (2019). The agreement between the two models encourages the adoption of remote sensing and video prediction-based UGPM to provide the city of Dubai's authorities and urban planners with adequate tools to predict the city's growth with limited data requirements.

5.2. Cairo, Egypt

The growth prediction results for the city of Cairo are presented in Fig. 7. The model predicts a steady growth towards the east and the west deserts as well as the disappearance of several agricultural pockets in the Nile's Delta. The growth in the east side of the city, identified by Zone 2 and Zone 3, extends Cairo's boundaries through a new development in the east known as New Cairo. This growth is supported by the accessibility provided by two main highways, namely, the Suez Rd. and the Ain El Sokhna Rd. It is worth mentioning that Egypt's government has recently announced the start of a mega-project to develop a New Administrative Capital (NAC) further east of New Cairo, which is planned as a modern city with a target population of 5.0 to 6.5 M people (Loewert & Steiner, 2019). This new administrative city is expected to expedite the growth on the east side of old Cairo predicted by the model. The model also predicts a similar growth in the western boundaries of Greater Cairo as depicted by Zone 5. This zone presents the development in New Giza, a new development west of the old Giza City (the western part of the Greater Cairo Metropolitan Area). This western growth is also promoted by the ongoing developments in the Sheikh Zayed City and the 6th of October City, which are relatively new cities located 30 miles from Cairo's downtown in the west desert, and the transportation infrastructure developed to connect the two cities to Cairo (e.g., Cairo's Ring Rd and Alexandria's Desert Rd.). The other two zones (Zone 1 and Zone 4) predict new developments on agricultural lands in the north and the south of the Niles's Delta. The growth of the city of Cairo on the expense of agricultural land is a trend that has been observed during the past few decades. The model predicts the disappearance of the agricultural lands in Al-Qalg area in Qalyubia (Zone 1), and Abo Al-Nomros area in Giza (Zone 4). Both zones include agricultural lands surrounded by very high-density residential areas that were also built on an agricultural land in the past two decades. We compared the obtained

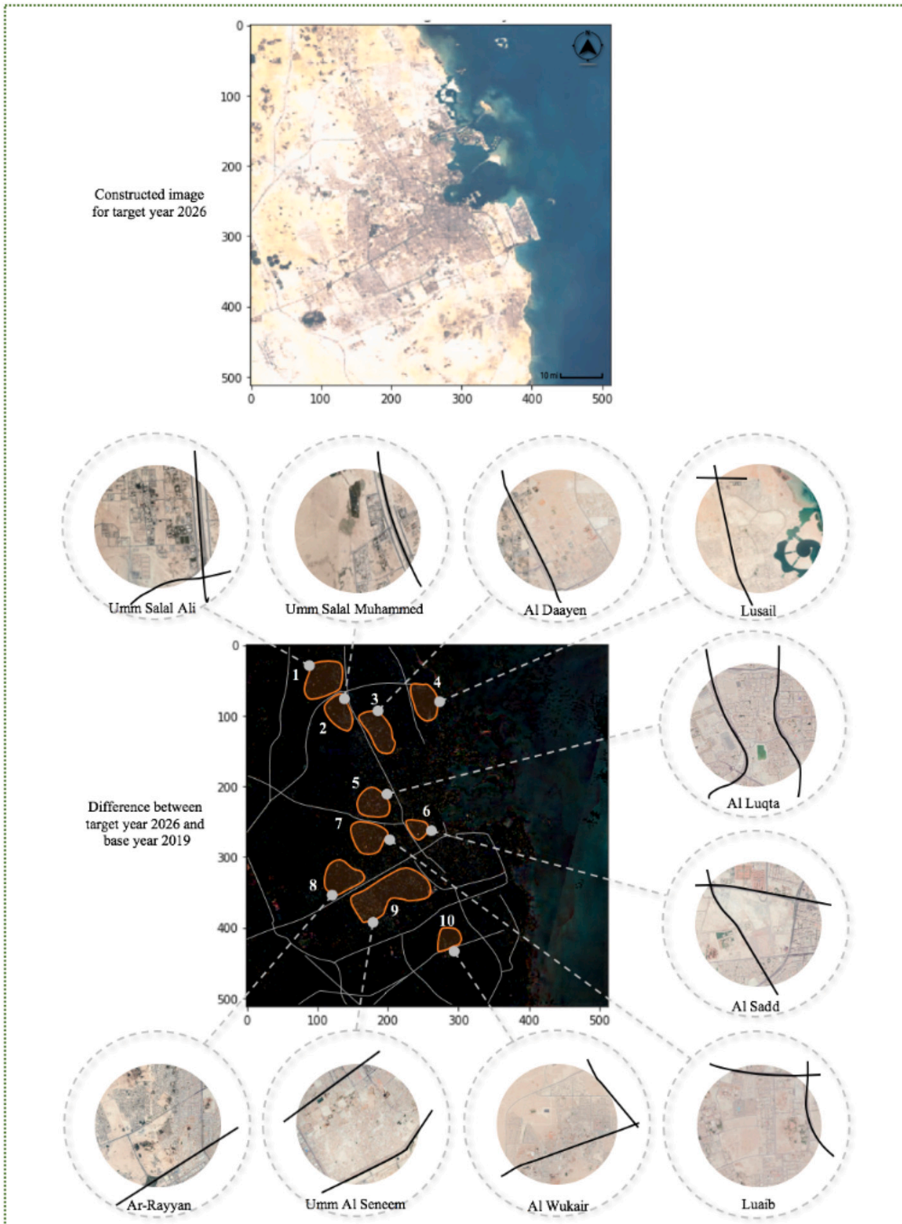

Fig. 8. Predicted urban growth of the city of Doha for year 2026.

prediction results with a previous study that reported the change in the urban extent of Cairo Metropolitan Area. The study gives a prediction of the open space for future urbanization, as given in Fig. 12 (Angel et al., 2012). This benchmarking study is based on a collaboration between the Urban Expansion Program at New York University, the United Nations Human Settlements Program (UN-Habitat), and the Lincoln Institute of Land Policy. The study is applied to a global sample of 200 cities (e.g., New York, Sydney, Montreal, Wuhan, Cairo, Riyadh) to map the spatial changes and urban expansion. The study adopts a data intensive approach, using data that were extracted from satellite images and land use surveys to predict the urban expansion of the city beyond 2013 with no specific target year. We superimposed the five growth zones predicted by the model on top of the urban expansion map reported in Angel et al. (2012). As shown in the figure, all these growth zones are coinciding with the predicted urban extent for the metropolitan area (indicated by the yellow color). As the benchmarking study does not define a specific target year, one would expect the results of this study to show urban expansion that is not identified by our model which limits its prediction to year 2026.

5.3. Doha, Qatar

Similar to the results presented above, Fig. 8 gives the constructed satellite image for the city of Doha in the target year. The figure also shows the difference between this constructed image and the base year's image, highlighting zones with predicted significant growth activities. As shown in the figure, ten growth zones are identified by the model. Most of these zones are falling in semi-urbanized space near the city's current boundaries. These predicted growth zones are well connected through a strong highway system. For example, a growth is predicted to occur towards the north side of the city as indicated by Zones 1 to 4, namely Umm Salal Ali, Umm Salal Muhammed, and Al-Daayen. These zones are located near main roadways in the city such as Wadi Al-Wasah Rd. and the Doha Expressway. Growth is also expected to occur on the west side as illustrated by Zones 5 to 9 in Al-Luqta, Luaib, Al-Rayyan, and Umm Al-Seneem areas. These areas can also be accessed by major

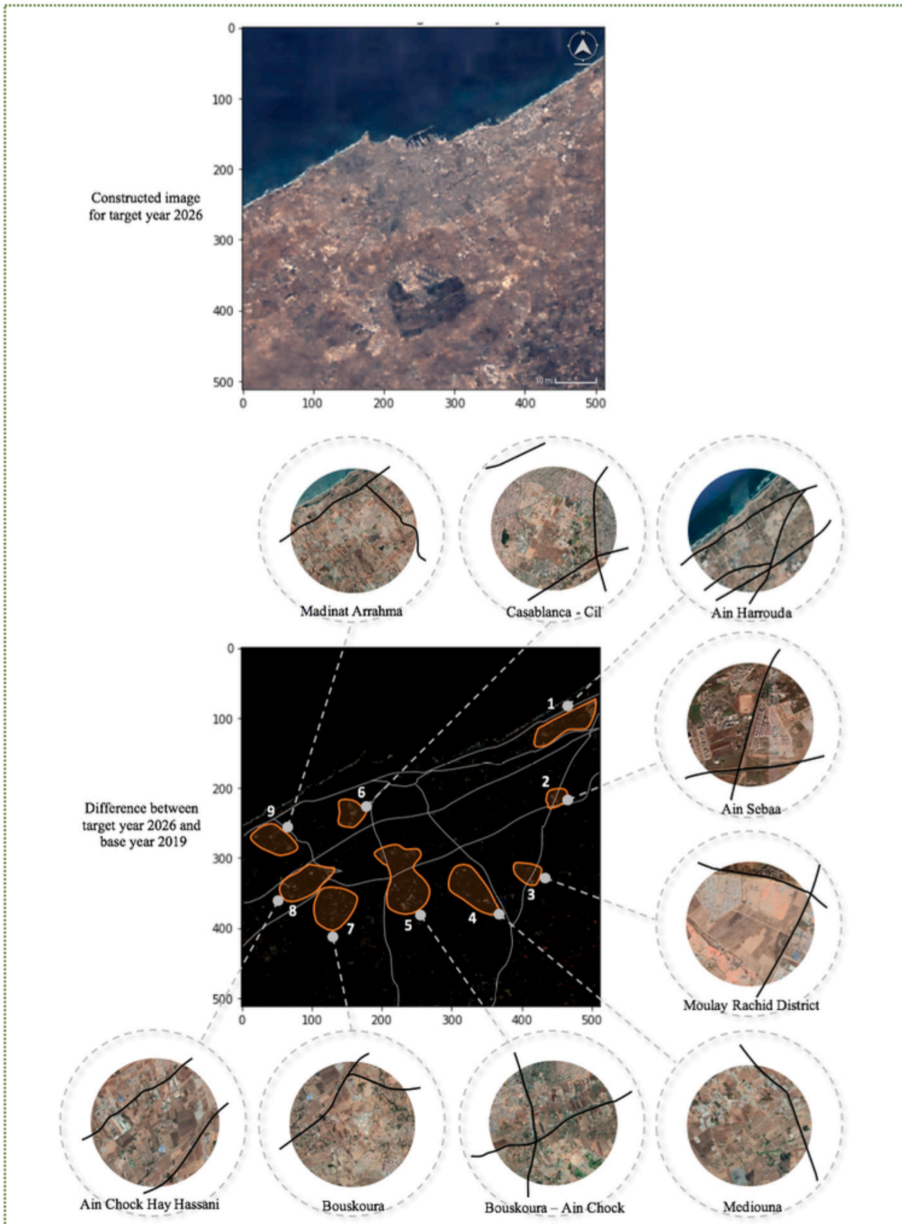

Fig. 9. Predicted urban growth of the city of Casablanca for year 2026.

roads that connect the city in the north-south and the east-west directions such as the Doha Expressway, Al-Rayyan Rd. and Salwa Rd. Finally, the model predicts growth in Zone 10 known as Al Wukair area located at the south side of the city. This zone extends the west side of the city of Al-Wakrah predicting its merge with the city of Doha, forming a large multi-city metropolitan area. Further investigating the locations of these zones and their surrounding environments, most of these zones are found to be located near mega commercial, entertainment, sport and education projects that are currently planned or under construction including Lusall, the Pearl, Katara, West Bay Area, Souq Wagif, Education City, and the Aspire Zone (Azzali, 2017). These results are compared against the growth pattern predicted by Makido et al. (2020). The approach adopted by Makido et al. (2020) is an empirical land-use change model that merges GIS with ANN to predict urban growth based on a set of representative variables (e.g., distance to roads, distance to previously developed areas, distance to urban center, and distance to the coast). The results of their model are presented in Fig. 13, which illustrates the urban growth predicted for target year 2028. The results obtained from our UGPM adopted is overlaid on that figure. On the north side, the growth predicted in Zones 2, 3 and 4 seems to agree with that predicted by Makido et al. (2020). However, the two models disagree with respect to the coastal growth on the north side of the city. Makido et al. (2020) predicted an expedited coastal growth at the north side that might not be realistic for target year 2028. On the south side, the two models agree in terms of the predicted growth for Zones 8 and 10, respectively. Other zones (Zones 5–7 and 9) predicted by the model suggest an increase in the development density within the current boundaries of the city, which was not depicted by the benchmarking model.

5.4. Casablanca, Morocco

The prediction results of the city of Casablanca are provided in Fig. 9. Similar to Dubai and Doha, the predicted growth is happening mostly inland and along the coast. However, two observations differentiate Casablanca from these two cities. First, all predicted growth zones are

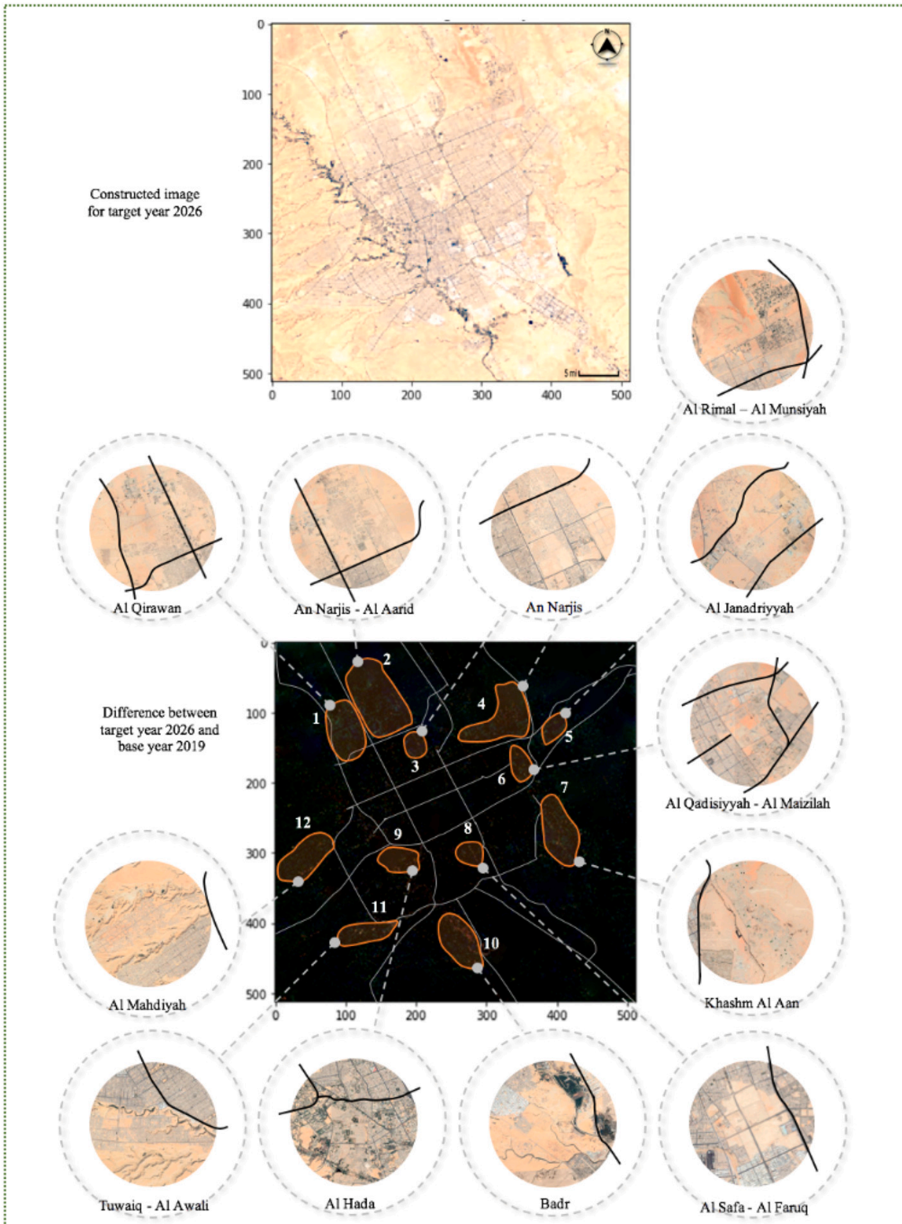

Fig. 10. Predicted urban growth of the city of Riyadh for year 2026.

located at the city's current boundaries. Such a pattern is expected as Casablanca is an older city that is highly developed with limited vacant land available inside the city's current boundaries. Second, the predicted peripheral growth is almost uniformly distributed around the city. The city's high population growth rates combined with the intensive labor migration from its surrounding farms could explain this predicted uniform peripheral growth (Mallouk et al., 2019). The increase in the population from inside the city and the migrating population from its surrounding farms are naturally meeting at the city's current boundaries and expediting its growth along these boundaries. As shown in the figure, nine growth zones are identified by the model. For example, Zone 1 predicts growth northeast of the city in Ain Harrouda, which is an ocean front area between the city of Casablanca and the city of Mohemmedia. Zones 2 and 3 are located in the east side of Casablanca (Ain Sebaa, and Moulay Rachid District). These zones are supported by strong highway connectivity including A1 and N9 highways. Similarly, Zones 4 and 5 known as Mediouna, Bouskoura, and Ain Chock predict a growth on the south side along highways R315 and N1, respectively. A significant growth is also predicted in the west side of the city (Zones 6–9) in the Casablanca-Cil, Bouskoura, Ain Chock Hay Hassani, and Madinat Arrahma areas, respectively. We compared our results against the growth pattern reported in Mallouk et al. (2019), which gives the probability of growth in year 2040 beyond the city's current boundaries, as illustrated in Fig. 14. This benchmarking study adopts the SLEUTH cellular automaton model Chaudhuri and Clarke (2013), which is calibrated using satellite images from 1984 and 2018. As shown in the figure, the two models agree in their predictions in most cases, especially in the northeast and the southwest sides of the city along the ocean front.

5.5. Riyadh, KSA

The growth prediction results obtained by the model for the city of Riyadh are presented in Fig. 10. Based on these results, the city is predicted to grow from all directions. Twelve growth zones are depicted in the figure. One can expect this growth pattern considering the following factors: (1) this peripheral growth pattern matches the historical growth

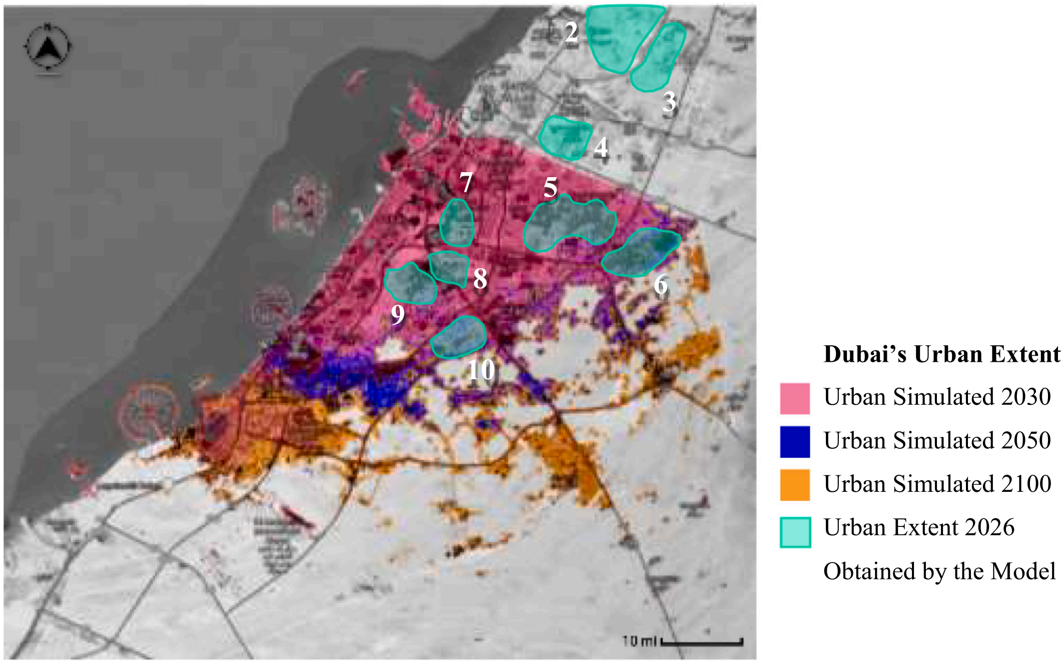

Fig. 11. Model validation and urban expansion of the city of Dubai.
(Source: Aldogom et al. (2019)).

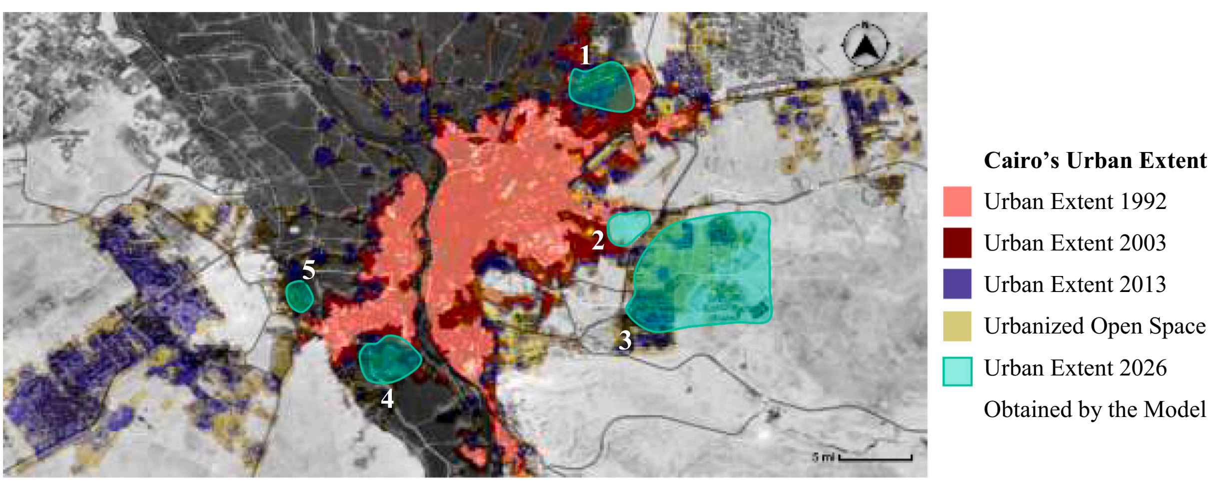

Fig. 12. Model validation and urban expansion of the city of Cairo.
(Source: Angel et al., 2012)

pattern observed for the city during the past few decades; (2) the city continues to experience high population growth with a strong cultural preference of single-family dwellings pushing for new developments outside the city limits where the land is generally cheaper; and (3) the city is characterized by flat topography in the surrounding desert which promotes such a growth pattern. For example, Zones 1 to 3 are the result of urban sprawl occurring in the north side of the city in the An-Narjis and Al-Aarid divisions. Such growth is also supported by the proximity to King Fahd Rd. and King Salman Rd. Zone 4, located in the northeast side of Al-Rimal and Al-Munsiyah divisions, is another area with predicted growth. The growth in this zone is supported by its proximity to Al-Janadriyah Rd. in the east and Dammam Rd. in the south. Another example is Zone 12, which is located on the west side of the city in the Al Mahdiyah area. This zone extends a fully developed area, Dhahrat Laban, further to the north. We compared the obtained prediction results with those of a previous study that predicts the change in the urban extent of the city of Riyadh, as given in Fig. 15 (Angel et al., 2012). Similar to the city of Cairo, this benchmarking study is a collaboration between the Urban Expansion Program at New York University, the United Nations Human Settlements Program (UN-Habitat), and the Lincoln Institute of Land Policy. It adopts a data intensive approach extracted from satellite images and land-use surveys to predict the urban expansion of the city beyond 2013 with no specific target year. In most cases, the growth zones predicted by the model match the city's reported urban extent in the benchmarking study. This match in the prediction results is more obvious in the north and the east sides of the city, where all predicted growth zones are falling in the urbanized open space predicted for the city.

6. Discussion and conclusion

Cities in the Middle East and North Africa (MENA) region have

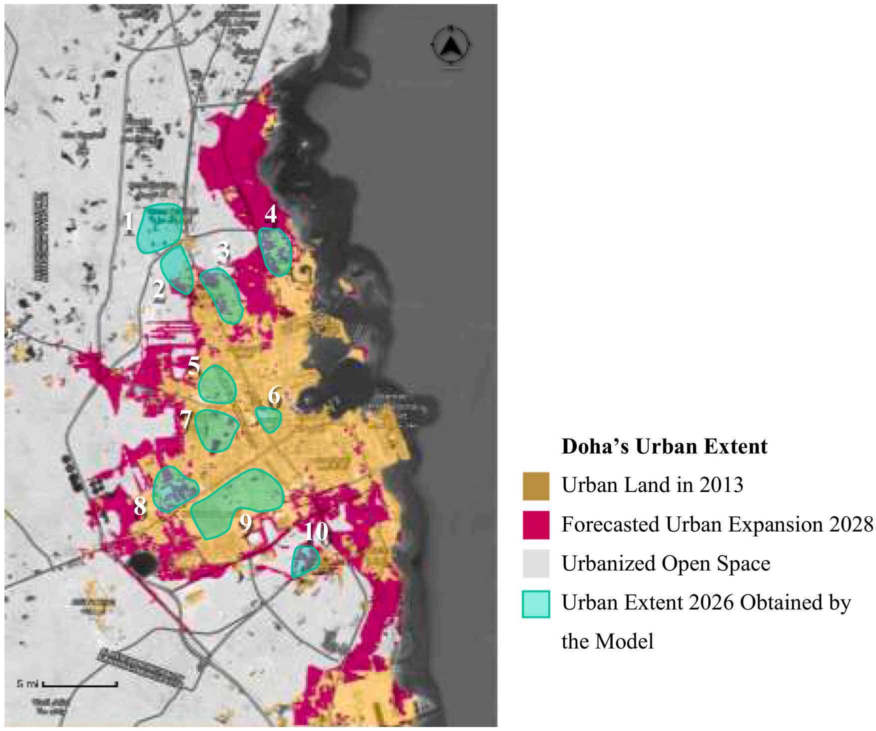

Fig. 13. Model validation and urban expansion of the city of Doha.
(Source: Makido et al., 2020)

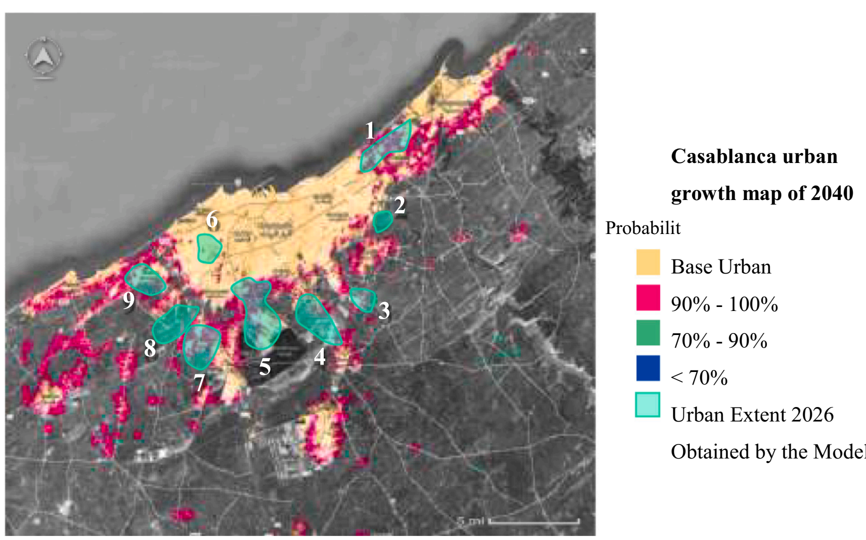

Fig. 14. Model validation and urban expansion of the city of Casablanca. (Source: Mallouk et al., 2019).

experienced significant population increase over the past few decades. As such, most urban areas in the region have expanded significantly to accommodate such population increase. Unfortunately, the expedited urbanization observed in most cities in the region presents substantial stresses to their ecological and financial resources, as well as to the overall well-being of their residents. To ensure long-term sustainability and eliminate the risk of uncontrolled growth in these cities, there have been increasing calls for adequate urban growth prediction studies that can be used as a foundation to develop sustainable growth plans for these cities. This paper studies the urban growth pattern in five major cities in the MENA region including Dubai (United Arab Emirates (UAE)), Cairo (Egypt), Doha (Qatar), Casablanca (Morocco), and Riyadh (Kingdom of Saudi Arabia (KSA)). These cities are a representative sample of cities in the region that differ in their size, population density, historical heritage, level of control applied to growth, geographical locations, complexity of their structure, and economic strength. The study adopts a machine learning (ML)-based modeling framework developed by the authors in a previous effort (Jaad & Abdelghany, 2020). The model integrates remote sensing and computer vision technologies to generate high-fidelity urban growth prediction with limited data requirements. The model treats a sequence of satellite images taken over an extended past horizon for the urban area under study as a video for which a future frame can be predicted representing the growth in the target year. The model is in the form of a time-dependent encoder-decoder (TDED) with embedded convolutional neural networks (CNN). The model is trained to learn the spatiotemporal growth features from

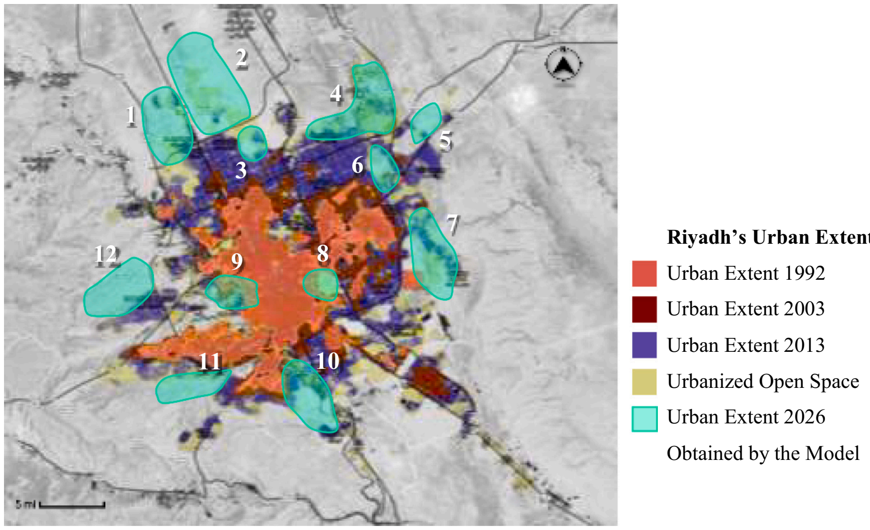

Fig. 15. Model validation and urban expansion of the city of Riyadh. (Source: Angel et al., 2012).

the satellite images, which enables it to predict the growth pattern in the urban area for a given future year. The input of a trained model includes: (a) a base-year satellite image with a pre-defined resolution for the urban area under study; and (b) the length of the prediction horizon of interest (i.e., target year). The model constructs an image that predicts the growth pattern for the urban area for the target year or any other year along the specified horizon. The prediction results obtained by the model are compared against the results collected from other urban growth studies conducted for the selected cities. These results illustrate the potential of the presented approach to develop UGPMs with high fidelity.

Based on the results obtained for these MENA cities, several recommendations can be derived to assist city planners and policy makers in the MENA region and in other parts of the world on their mission to develop sustainable urban growth plans for their cities. First, a strong correlation is observed between the roadway network and the predicted growth in all studied cities. Land developers usually give priority to vacant areas that are accessible by the existing roadway system. As such, the integration of the urban and transportation planning processes for urban areas is critical for ensuring their sustainable growth. In addition, while ring roads have been constructed to ease traffic congestion inside cities and to set rigid boundaries to curb growth, they have been shown to be ineffective in defining city boundaries and preventing its urban sprawl. For example, the city of Cairo continued to grow beyond its recently constructed ring road from almost all directions. This pattern has been also observed in other cities around the world (Juan, 2018). For example, the current roadway network of the city of Beijing, China includes seven ring roads which are developed over the past century aiming to confine the city size. These roads clearly failed to achieve that goal and currently provide additional capacity to the city's roadway network. Second, careful attention needs to be given to the planning of mega projects in urban areas. As these projects usually represent major attractions, they could result in significant changes in their surrounding areas, either in terms of new developments or a change in the current land-use. For example, most urban developments predicted in the city of Doha are triggered by nearby new mega projects planned in the city. Similar pattern is observed in other cities around the world, where mega projects have significantly impacted their surroundings (Higginbotham, 2014). For example, the Europa City is a major development north of Paris that includes 8.6-million-square-foot mixed-use development (Vinnitskaya, 2013). The project is expected to convert a largely rural area into a a mixed-use suburban area that is connected with urban Paris. The Europa City includes housing, shops, and restaurants, plazas, an artificial ski slope, open walkways, a golf system, and a new transit system. Third, there is always considerable benefits in diversifying housing options within the city to prevent urban sprawl. These housing options include apartment buildings and townhomes which create high density residential areas near business districts and transit services (e.g., transit-oriented developments). For example, the expedited urban sprawl observed in the city of Riyadh is primarily contributed to the high preference of most households to live in a single-family home, even in the case of small family sizes. Housing policies and incentives that encourage small households to live in apartment buildings and townhomes could help in curbing the sprawl observed in the city. Diversifying housing choices in urban area is proven to be effective strategy for ensuring community stability and controlling urban sprawl (Chakraborty & McMillan, 2018; Habibi & Asadi, 2011). Data from fourteen U.S. metropolitan areas showed that cities that are diversified in terms of their housing options have recorded less foreclosure cases during the recent housing crisis and less need for new housing production on the long run.

Fourth, most cities in the region are suffering heavy migration from surrounding rural areas. This migration is mainly due to increasing agricultural automation and the lack of alternative job opportunities for the traditional agricultural labor. As observed in the cities of Cairo and Casablanca, the migration of poor labor to nearby cities has resulted in the creation of slums and neighborhoods with no adequate services. As such, adequate economic investment is needed to create viable economic opportunities in the surrounding rural areas to reduce this migration and prevent its adverse consequences. This phenomenon is widely observed in many cities around the world (Afsar, 2003; Hu et al., 2008; Skeldon, 1997; Zhao, 1999). For instance, according to the UN 2018 statistics, rural-to-urban migration accounted for more than half of the growth in the urban areas of counties such as China and Thailand (80%), Rwanda (79%), Indonesia (68%) and Namibia (59%). These significant jump in these cities' population has resulted in unplanned growth indicated by slums and neighborhoods with inadequate infrastructure and services. Finally, urban growth could occur at the expense of valuable natural resources within or surrounding the city. For example, the city of Cairo has been growing at the expense of high-value agricultural land on the north and the south boundaries. Similarly, the growth in Dubai and Doha is reported to be occurring at the expense of green space within these cities. Unfortunately, growing urban areas on the expenses of high-value agricultural land and green spaces is a worldly trend (Cocklin et al., 1983; Krannich, 2006; Marin, 2007; Yunus, 1990). This trend has shown to have significant impact on food security and green space equity (Dinda et al., 2021; Dongol & Shrestha, 2017; Xu et al., 2018). As such, strict regulations and incentives are required to prevent such growth pattern to ensure that valuable natural resources are preserved (Conklin, 1976).

CRediT authorship contribution statement

Jaad: Data curation, Methodology, Software, Data curation, Experiment preparation, Visualization, Original draft preparation.

Abdelghany: Conceptualization, Methodology, Software, Writing-Reviewing and Editing.

Declaration of competing interest

The authors declare that they have no known competing financial interests or personal relationships that could have appeared to influence the work reported in this paper.

References

Abdalmalak, K. A., & Gonzalez-Serrano, F. J. (2016). Forecasting of Cairo population using ARMA model. *The Egyptian International Journal of Engineering Sciences & Technology, 19*(2), 346–352.

Abulibdeh, A., Al-Awadhi, T., & Al-Barwani, M. (2019). Comparative analysis of the driving forces and spatiotemporal patterns of urbanization in Muscat, Doha, and Dubai. *Development in Practice, 29*(5), 606–618.

Acharya, U. R., Oh, S. L., Hagiwara, Y., Tan, J. H., & Adeli, H. (2018). Deep convolutional neural network for the automated detection and diagnosis of seizure using EEG signals. *Computers in Biology and Medicine, 100*, 270–278.

Afsar, R. (2003). Internal migration and the development nexus: The case of Bangladesh. In *Regional conference on migration, development and pro-poor policy choices in Asia* (pp. 22–24).

Al-Ahmadi, K. (2018). Modeling driving forces of urban growth with fuzzy sets and GIS. In *Spatial analysis, modelling and planning*. IntechOpen.

Al-Ahmadi, K., Alahmadi, M., & Alahmadi, S. (2016). Spatial optimization of urban cellular automata model. Applications of spatial statistics. *INTECH*, 61–94.

Aldogom, D., Aburaed, N., Al-Saad, M., Al Mansoori, S., Al Shamsi, M. R., & Al Maazmi, A. A. (2019). Multi-temporal satellite images for growth detection and urban sprawl analysis; Dubai City, UAE. In *, Vol. 11157. Remote sensing technologies and applications in urban environments IV* (p. 111570). International Society for Optics and Photonics.

Alghais, N. (2018). *Developing urban models to address population growth impacts and assisting with future urban planning in Kuwait and other Arabian Gulf countries*.

Alghamdi, A., & Cummings, A. R. (2019). Assessing Riyadh's urban change utilizing high-resolution imagery. *Land, 8*(12), 193.

Alqurashi, A. F., Kumar, L., & Sinha, P. (2016). Urban land cover change modeling using time-series satellite images: A case study of urban growth in five cities of Saudi Arabia. *Remote Sensing, 8*(10), 838.

AlSayyad, N. (2013). *Cairo: Histories of a city*. Cambridge, Massachusetts, USA: The Belknap Press of Harvard University Press.

Altuwaijri, H. A., Alotaibi, M. H., Almudlaj, A. M., & Almalki, F. M. (2019). Predicting urban growth of arriyadh city, capital of the Kingdom of Saudi Arabia, using markov cellular automata in TerrSet geospatial system. *Arabian Journal of Geosciences, 12*(4), 135.

Angel, S., Parent, J., Civco, D. L., & Blei, A. M. (2012). *Atlas of urban expansion*. Cambridge MA: Lincoln Institute of Land Policy. www.lincolninst.edu/subcenters/atlas-urban-expansion.

Ayazli, I. E., Gul, F. K., Yakup, A. E., & Kotay, D. (2019). Extracting an urban growth model's land cover layer from spatio-temporal cadastral database and simulation application. *Polish Journal of Environmental Studies, 28*(3).

Azzali, S. (2017). Mega-events and urban planning: Doha as a case study. *Urban Design International, 22*(1), 3–12.

Azzali, S., & Tomba, M. (2018). Urban development and planning practice in Doha. *Mei Insight, 180*, 1–13.

Bang, S., Park, S., Kim, H., & Kim, H. (2019). Encoder–decoder network for pixel-level road crack detection in black-box images. *Computer-Aided Civil and Infrastructure Engineering, 34*(8), 713–727.

Berling-Wolff, S., & Wu, J. (2004). Modeling urban landscape dynamics: A case study in Phoenix, USA. *Urban Ecosystems, 7*(3), 215–240.

Black, K. M., Law, H., Aldouhki, A., Deng, J., & Ghani, K. R. (2020). *Deep learning computer vision algorithm for detecting kidney stone composition*. BJU International.

Brownlee, J. (2016). *Deep learning with python: Develop deep learning models on Theano and TensorFlow using Keras*. Machine Learning Mastery.

Bugday, E., & Bugday, S. E. (2019). Modeling and simulating land use/cover change using artificial neural network from remotely sensing data. *Cerne, 25*(2), 246–254.

Chakraborty, A., & McMillan, A. (2018). Is housing diversity good for community stability?: Evidence from the housing crisis. *Journal of Planning Education and Research*, 0739456X18810787.

Chaudhuri, G., & Clarke, K. (2013). The SLEUTH land use change model: A review. *Environmental Resources Research, 1*(1), 88–105.

Chauvin, Y., & Rumelhart, D. E. (2013). *Backpropagation: Theory, architectures, and applications*. Oxfordshire, England: Psychology Press.

Chen, S., Leng, Y., & Labi, S. (2020). A deep learning algorithm for simulating autonomous driving considering prior knowledge and temporal information. *Computer-Aided Civil and Infrastructure Engineering, 35*(4), 305–321.

Cho, C., Park, J., & Sakhakarmi, S. (2019). Emergency response: Effect of human detection resolution on risks during indoor mass shooting events. *Safety Science, 114*, 160–170.

Choi, J., & Dyke, S. J. (2020). CrowdLIM: Crowdsourcing to enable lifecycle infrastructure management. *Computers in Industry, 115*, Article 103185.

Clarke, K. C., & Gaydos, L. J. (1998). Loose coupling a cellular automaton model and GIS: Long-term urban growth prediction for San Francisco and Washington/Baltimore. *International Journal of Geographical Information Science, 12*(7), 699–714.

Cocklin, C., Gray, E., & Smit, B. (1983). Future urban growth and agricultural land in Ontario. *Applied Geography, 3*(2), 91–104.

Conklin, H. E. (1976). *Property tax incentives to preserve farming in areas of urban pressure (No. 641-2016-43534*.

Dinda, S., Chatterjee, N. D., & Ghosh, S. (2021). An integrated simulation approach to the assessment of urban growth pattern and loss in urban green space in Kolkata, India: A GIS-based analysis. *Ecological Indicators, 121*, Article 107178.

Dongol, R., & Shrestha, R. (2017). Land use change due to urbanization and its impact on local food security: Case of MadhyapurThimi Municipality. In *Paper presentation in International Conference on Sustainable Development at Dhaka*.

Elessawy, F. (2017). The boom: population and urban growth of Dubai City. *Horizons Hum. Soc. Sci, 2*, 26–41.

Elmahdy, S. I., & Mohamed, M. M. (2018). Monitoring and analyzing the emirate of Dubai's land use/land cover changes: An integrated, low-cost remote sensing approach. *International Journal of Digital Earth, 11*(11), 1132–1150.

Elsheshtawy, Y. (2019). Transforming Riyadh: A new urban paradigm? The Arab Gulf States Institute in Washington. Retrieved from https://agsiw.org/.

Folkers, A. S., & Buiten, B. (2019). *Modern architecture in Africa: Practical encounters with intricate African modernity*. Cham, Switzerland: springer Nature.

Gao, Y., & Mosalam, K. M. (2018). Deep transfer learning for imagebased structural damage recognition. *Computer-Aided Civil and Infrastructure Engineering, 33*(9), 748–768.

Gerasimovic, M., Bugaric, U., & Božic, M. (2016). Enrollment management: Development of prediction model based on logistic regression. *FME Transactions, 44*(1), 92–98.

Gómez, J. A., Patiño, J. E., Duque, J. C., & Passos, S. (2020). Spatiotemporal modeling of urban growth using machine learning. *Remote Sensing, 12*(1), 109.

Gouda, A. A., Hosseini, M., & Masoumi, H. E. (2016). The status of urban and suburban sprawl in Egypt and Iran. *GeoScape, 10*, 1–15.

Habibi, S., & Asadi, N. (2011). Causes, results and methods of controlling urban sprawl. *Procedia Engineering, 21*, 133–141.

Han, Y., & Jia, H. (2017). Simulating the spatial dynamics of urban growth with an integrated modeling approach: a case study of Foshan, China. *Ecological Modelling, 353*, 107–116.

Hashem, N., & Balakrishnan, P. (2015). Change analysis of land use/land cover and modelling urban growth in greater Doha. *Qatar. Annals of GIS, 21*(3), 233–247.

Hashemi, H., & Abdelghany, K. (2018). End-to-end deep learning methodology for real-time traffic network management. *Computer-Aided Civil and Infrastructure Engineering, 33*(10), 849–863.

He, C., Okada, N., Zhang, Q., Shi, P., & Zhang, J. (2006). Modeling urban expansion scenarios by coupling cellular automata model and system dynamic model in Beijing, China. *Applied Geography, 26*(34), 323–345.

He, K., Zhang, X., Ren, S., & Sun, J. (2016). Deep residual learning for image recognition. In *Proceedings of the IEEE conference on computer vision and pattern recognition* (pp. 770–778). Piscataway, NJ: Institute of Electrical and Electronics Engineers Inc.

Held, C. C., & Cummings, J. T. (2018). *Middle East patterns, student economy edition: Places, people, and politics* (6th ed.). Routledge.

Higginbotham, J. (2014). 9 mega redevelopments poised to transform the urban landscape. Online Access June 2021. In *Smart and resilient cities* https://www.bdcnetwork.com/9-mega-redevelopments-poised-transform-urban-landscape.

Hu, X., Cook, S., & Salazar, M. A. (2008). Internal migration and health in China. *The Lancet, 372*(9651), 1717–1719.

Husodo, A. Y., Jati, G., Alfiany, N., & Jatmiko, W. (2019). Intruder drone localization based on 2Dimage and area expansion principle for supporting military defence system. In *2019 IEEE international conference on communication, networks and satellite (Comnetsat)* (pp. 35–40). IEEE.

Ibrahim, M. R., Titheridge, H., Cheng, T., & Haworth, J. (2019). predictSLUMS: A new model for identifying and predicting informal settlements and slums in cities from street intersections using machine learning. *Computers, Environment and Urban Systems, 76*, 31–56.

International Centre for Migration Policy Development (ICMPD). (2018). City migration profile amman -executive summary. https://www.icmpd.org/fileadmin/1_2018/MC2CM/City_Migration_Profile_Amman_EN.pdf. Access Date April, 2020.

Jaad, A., & Abdelghany, K. (2020). Modeling urban growth using video prediction technology: A time-dependent convolutional encoder–decoder architecture. *Computer-Aided Civil and Infrastructure Engineering, 35*, 430–447.

Joubert, N., Reid, T. G., & Noble, F. (2020). *Developments in modern GNSS and its impact on autonomous vehicle architectures*. arXiv preprint arXiv:2002.00339.

Juan, D. (2018). *Construction completed on Beijing's '7th Ring Road*. June 21, 2018. Online Access June 2021. China Daily http://www.chinadaily.com.cn/a/201806/21/WS5b2addc8a3103349141dd653.html.

Kadhim, N., Mourshed, M., & Bray, M. (2016). Advances in remote sensing applications for urban sustainability. *Euro-Mediterranean Journal for Environmental Integration, 1*(1), 7.

Kalinin, A. A., Iglovikov, V. I., Rakhlin, A., & Shvets, A. A. (2020). Medical image segmentation using deep neural networks with pre-trained encoders. In *Deep learning applications* (pp. 39–52). Singapore: Springer.

Kaur, P., & Khosla, P. K. (2020). Artificial intelligence based glaucoma detection. In *Advancement of machine intelligence in interactive medical image analysis* (pp. 283–305). Singapore: Springer.

Ke, X., Qi, L., & Zeng, C. (2016). A partitioned and asynchronous cellular automata model for urban growth simulation. *International Journal of Geographical Information Science, 30*(4), 637–659.

Khalil, M. A., Al-Ruzouq, R., Hamad, K., & Shanableh, A. (2017). Multi-temporal satellite imagery for infrastructure growth assessment of Dubai City, UAE. In *, Vol. 120. MATEC web of conferences* (p. 09006). EDP Sciences.

Krannich, J. M. (2006). A modern disaster: agricultural land, urban growth, and the need for a federally organized comprehensive land use planning model. *Cornell JL & Pub. Pol'y, 16*, 57.

LeCun, Y., Bengio, Y., & Hinton, G. (2015). Deep learning. *Nature, 521*(7553), 436–444.

Li, J., Wang, C., Kang, X., & Zhao, Q. (2019). Camera localization for augmented reality and indoor positioning: a vision-based 3D feature database approach. *International Journal of Digital Earth*, 1–15.

Liang, Y., Liu, L., & Huang, J. (2020). Modeling urban growth with CA model at regional scale. In *Integrated modelling of ecosystem services and land-use change* (pp. 19–38). Singapore: Springer.

Lin, Y. P., Chu, H. J., Wu, C. F., & Verburg, P. H. (2011). Predictive ability of logistic regression, auto-logistic regression and neural network models in empirical land-use change modeling—A case study. *International Journal of Geographical Information Science, 25*(1), 65–87.

Liu, W., & Seto, K. C. (2008). Using the ART-MMAP neural network to model and predict urban growth: A spatiotemporal data mining approach. *Environment and Planning B: Planning and Design, 35*(2), 296–317.

Loewert, P., & Steiner, C. (2019). The new administrative Capital in Egypt: The political economy of the production of urban spaces in Cairo. *Middle East-Topics & Arguments, 12*, 66–75.

Makido, Y., Shandas, V., & Ferwati, S. (2020). Predicting urban growth. In *Urban adaptation to climate change* (pp. 75–92). Cham: Springer.

Mallouk, A., Elhadrachi, H., Malaainine, M. E. I., Rhinane, H., & des Travaux Publics, E. H. (2019). Using the SLEUTH urban growth model coupled with a GIS to simulate and predict the future urban expansion of Casablanca region, Morocco. In *International archives of the photogrammetry, remote sensing and spatial information sciences* (p. 42) (4/W12).

Mansour, S., Al-Belushi, M., & Al-Awadhi, T. (2020). Monitoring land use and land cover changes in the mountainous cities of Oman using GIS and CA-markov modeling techniques. *Land Use Policy, 91*, Article 104414.

Marin, M. C. (2007). Impacts of urban growth boundary versus exclusive farm use zoning on agricultural land uses. *Urban Affairs Review, 43*(2), 199–220.

Midekisa, A., Holl, F., Savory, D. J., Andrade-Pacheco, R., Gething, P. W., Bennett, A., & Sturrock, H. J. (2017). Mapping land cover change over continental Africa using landsat and Google earth engine cloud computing. *PLoS One, 12*(9).

Mustafa, A., Cools, M., Saadi, I., & Teller, J. (2017). Coupling agentbased, cellular automata and logistic regression into a hybrid urban expansion model (HUEM). *Land Use Policy, 69*, 529–540.

New World Encyclopedia. (2016). Cairo. Retrieved fr https://www.newworldencyclopedia.org/entry/.

Osman, T., Divigalpitiya, P., & Arima, T. (2016). Using the SLEUTH urban growth model to simulate the impacts of future policy scenarios on land use in the Giza governorate, greater Cairo metropolitan region. *International Journal of Urban Sciences, 20*(3), 407–426.

Osman, T., Shaw, D., & Kenawy, E. (2019). An integrated land-use change model to simulate and predict the future of greater Cairo metropolitan region. *Journal of Land Use Science, 13*(6), 565–584.

Pijanowski, B. C., Pithadia, S., Shellito, B. A., & Alexandridis, K. (2005). Calibrating a neural network-based urban change model for two metropolitan areas of the upper Midwest of the United States. *International Journal of Geographical Information Science, 19*(2), 197–215.

Plecher, H. (2019). International. https://www.statista.com/markets/422/international/.

Qiu, S., Liu, Q., Zhou, S., & Wu, C. (2019). Review of artificial intelligence adversarial attack and defense technologies. *Applied Sciences, 9*(5), 909.

Rafiei, M. H., & Adeli, H. (2018). A novel unsupervised deep learning model for global and local health condition assessment of structures. *Engineering Structures, 156*, 598–607.

Saadani, S., Laajaj, R., Maanan, M., Rhinane, H., & Aaroud, A. (2020). Simulating spatial-temporal urban growth of a moroccan metropolitan using CA–Markov model. *Spatial Information Research*, 1–13.

Schmidhuber, J. (2015). Deep learning in neural networks: An overview. *Neural Networks, 61*, 85–117.

Shafizadeh-Moghadam, H., Asghari, A., Tayyebi, A., & Taleai, M. (2017). Coupling machine learning, tree-based and statistical models with cellular automata to simulate urban growth. *Computers, Environment and Urban Systems, 64*, 297–308.

Shandas, V., Makido, Y., & Ferwati, S. (2017). Rapid urban growth and land use patterns in Doha, Qatar: Opportunities for sustainability? *European Journal of Sustainable Development Research, 1*(11), 1–14. https://doi.org/10.20897/ejosdr.201711.

Shanmugamani, R. (2018). *Deep learning for computer vision: expert techniques to train advanced neural networks using TensorFlow and Keras*. Packt Publishing Ltd.

Skeldon, R. (1997). Rural-to-urban migration and its implications for poverty alleviation. *Asia-Pacific Population Journal, 12*(1), 3–16.

Statista Research Department. (2020). MENA: total population 2100. Retrieved from https://www.statista.com/statistics/978535/mena-total-population/#statisticContainer.

Tatarchenko, M., Dosovitskiy, A., & Brox, T. (2016). Multi-view 3d models from single images with a convolutional network. In *European conference on computer vision* (pp. 322–337). Cham: Springer.

Tayyebi, A., & Pijanowski, B. C. (2014). Modeling multiple land use changes using ANN, CART and MARS: Comparing tradeoffs in goodness of fit and explanatory power of data mining tools. *International Journal of Applied Earth Observation and Geoinformation, 28*, 102–116.

Tayyebi, A., Pijanowski, B. C., & Tayyebi, A. H. (2011). An urban growth boundary model using neural networks, GIS and radial parameterization: an application to Tehran, Iran. *Landscape and Urban Planning, 100*(1–2), 35–44.

Thakurdesai, H. M., & Aghav, J. V. (2020). Computer vision based position and speed estimation for accident avoidance in driverless cars. In *ICT Systems and Sustainability* (pp. 435–443). Singapore: Springer.

Thapa, R., & Murayama, Y. (2009). Examining spatiotemporal urbanization patterns in Kathmandu Valley, Nepal: Remote sensing and spatial metrics approaches. *Remote Sensing, 1*(3), 534–556.

The G-LUM Model. (2009). Predicting future spatial distributions of employment and households. Retrieved from http://www.ce.utexas.edu/prof/kockelman/G-LUM_Website/homepage.htm.

The UPLAN Model and Data. (2001). A detailed description of the UPLAN model. Retrieved from http://www.des.ucdavis.edu/faculty/johnston/pub7.htm.

Triantakonstantis, D., & Mountrakis, G. (2012). Urban growth predic- tion: A review of computational models and human perceptions. *Journal of Geographic Information System, 4*(6), 555–587.

U.S. Geological Survey. (2020). Landsat-earth observation satellites. Retrieved from https://pubs.er.usgs.gov/publication/fs20153081.

Ulrichsen, K. C. (2016). *The United Arab Emirates: Power, politics and policy making*. Taylor & Francis.

Van Vliet, J., White, R., & Dragicevic, S. (2009). Modeling urban growth using a variable grid cellular automaton. *Computers, Environment and Urban Systems, 33*(1), 35–43.

Verbeek, W. (2017). *Estimating the impacts of urban growth on future flood risk: A comparative study*. CRC Press.

Vinnitskaya, I. (2013). *BIG Wins Europa city development in Paris*. Access June 2021. ArcDaily Online https://www.archdaily.com/359796/big-design-wins-europe-city-development-in-paris.

Vukotic, V., Pintea, S. L., Raymond, C., Gravier, G., & van Gemert, J. C. (2017). One-step time-dependent future video frame prediction with a convolutional encoder-decoder neural network. In *International conference on image analysis and processing* (pp. 140–151). Cham: Springer.

Waddell, P. (2002). UrbanSim: Modeling urban development for land use, transportation, and environmental planning. *Journal of the American Planning Association, 68*(3), 297–314.

Wang, C., Dai, Y., Zhou, W., & Geng, Y. (2020). A Vision-Based Video Crash Detection Framework for Mixed Traffic Flow Environment Considering Low-Visibility Condition. *Journal of Advanced Transportation, 2020*. https://doi.org/10.1155/2020/9194028, 9194028.

Wang, Z., Bovik, A. C., Sheik, H. R., & Simoncelli, E. P. (2004). Image quality assessment: from error visibility to structural similarity. *IEEE Transactions on Image Processing, 13*(4), 1–14.

Weng, Q. (2002). Land use change analysis in the Zhujiang Delta of China using satellite remote sensing, GIS and stochastic modelling. *Journal of Environmental Management, 64*(3), 273–284.

Xu, C., Haase, D., Pribadi, D. O., & Pauleit, S. (2018). Spatial variation of green space equity and its relation with urban dynamics: A case study in the region of Munich. *Ecological Indicators, 93*, 512–523.

Ye, X. W., Jin, T., & Ang, P. P. (2020). Computer vision-based monitoring of ship navigation for bridge collision risk assessment. In *Machine vision and navigation* (pp. 787–807). Cham: Springer.

Yunus, H. S. (1990). Searching new strategies for managing and controlling urban land growth: A preliminary outlook on Indonesia. *Indonesian Journal of Geography, 20*(60), 1–10.

Zaina, S., Zaina, S., & Furlan, R. (2016). Urban planning in Qatar: Strategies and vision for the development of transit villages in Doha. *Australian Planner, 1–18*. https://doi.org/10.1080/07293682.2016.1259245.

Zhang, W., & Goh, A. T. (2016). Multivariate adaptive regression splines and neural network models for prediction of pile drivability. *Geoscience Frontiers, 7*(1), 45–52.

Zhao, Y. (1999). Leaving the countryside: Rural-to-urban migration decisions in China. *American Economic Review, 89*(2), 281–286.

Zhou, X., & Chen, H. (2018). Impact of urbanization-related land use land cover changes and urban morphology changes on the urban heat island phenomenon. *Science of the Total Environment, 635*, 1467–1476.